



Calhoun: The NPS Institutional Archive
DSpace Repository

Theses and Dissertations

1. Thesis and Dissertation Collection, all items

1976

Impedance measurement of the crossed-monopole wire structures.

Rundall, David G.

Monterey, California. Naval Postgraduate School

<http://hdl.handle.net/10945/17806>

Downloaded from NPS Archive: Calhoun



<http://www.nps.edu/library>

Calhoun is the Naval Postgraduate School's public access digital repository for research materials and institutional publications created by the NPS community. Calhoun is named for Professor of Mathematics Guy K. Calhoun, NPS's first appointed -- and published -- scholarly author.

Dudley Knox Library / Naval Postgraduate School
411 Dyer Road / 1 University Circle
Monterey, California USA 93943

IMPEDANCE MEASUREMENT OF THE
CROSSED-MONOPOLE WIRE STRUCTURES

David G. Rundall

NAVAL POSTGRADUATE SCHOOL

Monterey, California



THESIS

IMPEDANCE MEASUREMENT OF THE
CROSSED-MONOPOLE WIRE STRUCTURE

by

David G. Rundall

December 1976

Thesis Advisor:

Robert W. Burton

Approved for public release; distribution unlimited.

Prepared for: Air Force Weapons Laboratory/PRP
Kirtland AFB
New Mexico 87117

T176656

| REPORT DOCUMENTATION PAGE | | READ INSTRUCTIONS BEFORE COMPLETING FORM |
|--|-----------------------|--|
| 1. REPORT NUMBER NPS62Zn76122 | 2. GOVT ACCESSION NO. | 3. RECIPIENT'S CATALOG NUMBER |
| 4. TITLE (and Subtitle) Impedance measurement of the Crossed-Monopole Wire Structures | | 5. TYPE OF REPORT & PERIOD COVERED Final Report 29 March - 15 Dec 76 |
| | | 6. PERFORMING ORG. REPORT NUMBER |
| 7. AUTHOR(s) David G. Rundall | | 8. CONTRACT OR GRANT NUMBER(s) |
| 9. PERFORMING ORGANIZATION NAME AND ADDRESS Naval Postgraduate School Monterey, California 93940 | | 10. PROGRAM ELEMENT, PROJECT, TASK AREA & WORK UNIT NUMBERS |
| 11. CONTROLLING OFFICE NAME AND ADDRESS Air Force Weapons Laboratory/PRP Kirtland AFB New Mexico 87117 | | 12. REPORT DATE December 1976 |
| | | 13. NUMBER OF PAGES 121 |
| 14. MONITORING AGENCY NAME & ADDRESS (if different from Controlling Office) | | 15. SECURITY CLASS. (of this report) Unclassified |
| | | 15a. DECLASSIFICATION/DOWNGRADING SCHEDULE |
| 16. DISTRIBUTION STATEMENT (of this Report) Approved for public release, distribution unlimited. | | |
| 17. DISTRIBUTION STATEMENT (of the abstract entered in Block 20, if different from Report) | | |
| 18. SUPPLEMENTARY NOTES | | |
| 19. KEY WORDS (Continue on reverse side if necessary and identify by block number) Impedance Measurement Crossed-Monopole | | |
| 20. ABSTRACT (Continue on reverse side if necessary and identify by block number) This investigation experimentally determines the input impedance characteristics of various cylindrical crossed-monopole antennas at 2-12 GHz frequencies and compares the results to the well known characteristics of the cylindrical | | |

monopole antenna. The analysis includes a physical reasoning for the loading effects of the arms on the crossed-monopole antenna and resonance effects contributed by various members. The experimental results are also compared to the results obtained using numerical analysis.

Impedance Measurement of
the Crossed-Monopole Wire Structures

by

David G. Rundall
Lieutenant, United States Navy
B.S. (E.E.) University of Colorado, 1970

Submitted in partial fulfillment of the
requirements for the degree of

MASTER OF SCIENCE IN ELECTRICAL ENGINEERING

from the
NAVAL POSTGRADUATE SCHOOL
December 1976

Thesis

R863

c-1

NAVAL POSTGRADUATE SCHOOL
Monterey, California

Rear Admiral Isham W. Linder
Superintendent

Jack R. Borsting
Provost

This thesis was prepared in conjunction with research supported in part by AFWL/PRP under Project numbers 75-002 and 76-211. Reproduction of all or part of this report is authorized.

Released as a
technical report by:

UNITED STATES DEPARTMENT OF THE INTERIOR
BUREAU OF LAND MANAGEMENT

WATER RESOURCES DIVISION
SALT LAKE CITY, UTAH

ABSTRACT

This investigation experimentally determines the input impedance characteristics of various cylindrical crossed-monopole antennas at 2-12 GHz frequencies and compares the results to the well known characteristics of the cylindrical monopole antenna. The analysis includes a physical reasoning for the loading effect of the arms on the cross-monopole antenna and resonance effects contributed by various members. The experimental results are also compared to the results obtained using numerical analysis.

TABLE OF CONTENTS

| | | |
|------|--------------------------------------|----|
| I. | INTRODUCTION..... | 8 |
| A. | BACKGROUND..... | 8 |
| B. | THESIS OBJECTIVE..... | 9 |
| II. | THEORY..... | 10 |
| A. | MONOPOLES..... | 10 |
| B. | CROSSED-MONOPOLES..... | 15 |
| 1. | As a Loaded Monopole..... | 15 |
| 2. | Charge and Current Distribution..... | 17 |
| III. | EXPERIMENTAL EQUIPMENT..... | 21 |
| A. | WIRE STRUCTURES..... | 21 |
| B. | TEST FIXTURE..... | 24 |
| 1. | Female Adapter..... | 24 |
| 2. | Ground Plane..... | 25 |
| 3. | Anechoic Chamber..... | 27 |
| C. | MEASUREMENT SYSTEM..... | 28 |
| 1. | Configuration..... | 28 |
| 2. | Operation..... | 31 |
| 3. | Calibration..... | 32 |
| 4. | Accuracy..... | 43 |

| | | |
|-----|--|----|
| IV. | EXPERIMENTAL PROCEDURE..... | 45 |
| A. | DATA ACQUISITION..... | 45 |
| B. | DATA PROCESSING..... | 46 |
| C. | DATA ACCURACY..... | 46 |
| V. | EXPERIMENTAL RESULTS AND ANALYSIS..... | 51 |
| A. | MONOPOLES..... | 51 |
| 1. | 21 mm Monopole..... | 52 |
| 2. | 30 mm Monopole..... | 54 |
| 3. | 39 mm Monopole..... | 56 |
| 4. | 48 mm Monopole..... | 56 |
| B. | CROSSED-MONOPOLES..... | 60 |
| 1. | Case 1..... | 60 |
| 2. | Case 2..... | 65 |
| 3. | Case 3..... | 67 |
| 4. | Case 4..... | 69 |
| 5. | Case 5..... | 72 |
| 6. | Case 6..... | 74 |
| 7. | Case 7..... | 76 |
| 8. | Case 8..... | 79 |
| 9. | Case 9..... | 82 |
| 10. | Case 10..... | 84 |
| 11. | Case 11..... | 84 |
| 12. | Case 12..... | 88 |
| 13. | Case 13..... | 90 |

| | |
|--|-----|
| 14. Case 14..... | 93 |
| 15. Case 15..... | 95 |
| 16. Case 16..... | 97 |
| 17. Case 17..... | 101 |
| 18. Case 18..... | 103 |
| 19. Case 19..... | 106 |
| 20. Case 20..... | 108 |
| VI. COMPARISON OF EXPERIMENTAL RESULTS WITH NUMERICAL ANALYSIS..... | 110 |
| A. MONOPOLE..... | 110 |
| B. CROSSED-MONOPOLE..... | 113 |
| VII. CONCLUSIONS..... | 116 |
| LIST OF REFERENCES | 118 |
| INITIAL DISTRIBUTION LIST..... | 120 |

I. INTRODUCTION

A. BACKGROUND

The characteristics of straight cylindrical antennas are well known [King 1946]. Early work in this area focussed on electrically thin cylindrical dipoles over a lossless, infinite ground plane. Later theory expanded on these ideal conditions, but remained centered on primitive shapes due to the complexity of the problem. A growing body of experimental data on more complex configurations has provided the basis for greater understanding.

Interest in the crossed-dipole receiving antenna has been stimulated by modeling an aircraft in an Electromagnetic Pulse (EMP) environment as a crossed-dipole. Experimental measurements on thin crossed antennas in a plane-wave electromagnetic field [Burton 1974; Burton and King 1975] have shown the charge and current distributions, and the analytical investigation [King and Wu 1975] gives

further insight into the problem.

Since crossed-structures (either as a model for aircraft or physical structures on board ships) exist in considerable numbers, it is of interest to determine the transmitting characteristics of crossed-monopoles. The charge and current distributions of the transmitting crossed-monopole antenna [Mc Dowell 1976] have been measured, and reasoning developed in the analysis of the receiving crossed-dipole has been applied to the transmitting case with considerable success.

B. THESIS OBJECTIVE

The major objectives of this work were to experimentally determine the input impedance characteristics of various crossed-monopole antennas, compare the results with the input impedance of comparable monopole antennas, and give physical reasoning of the loading effects of the arms on the crossed-monopole antennas. The secondary objective was to compare the results with those obtained by using numerical analysis.

II. THEORY

A. MONOPOLE

The input impedance characteristics of a monopole antenna over a perfectly conducting ground plane are tabulated and graphs are available [Jordan and Balmain 1968]. Figure 1 shows a plot of the theoretical input resistance and reactance versus height-to-wavelength ratio for a monopole with a height-to-radius ratio of 60. Of particular interest are the peaks of the resistance curve and the zero-crossings of the reactance curve.

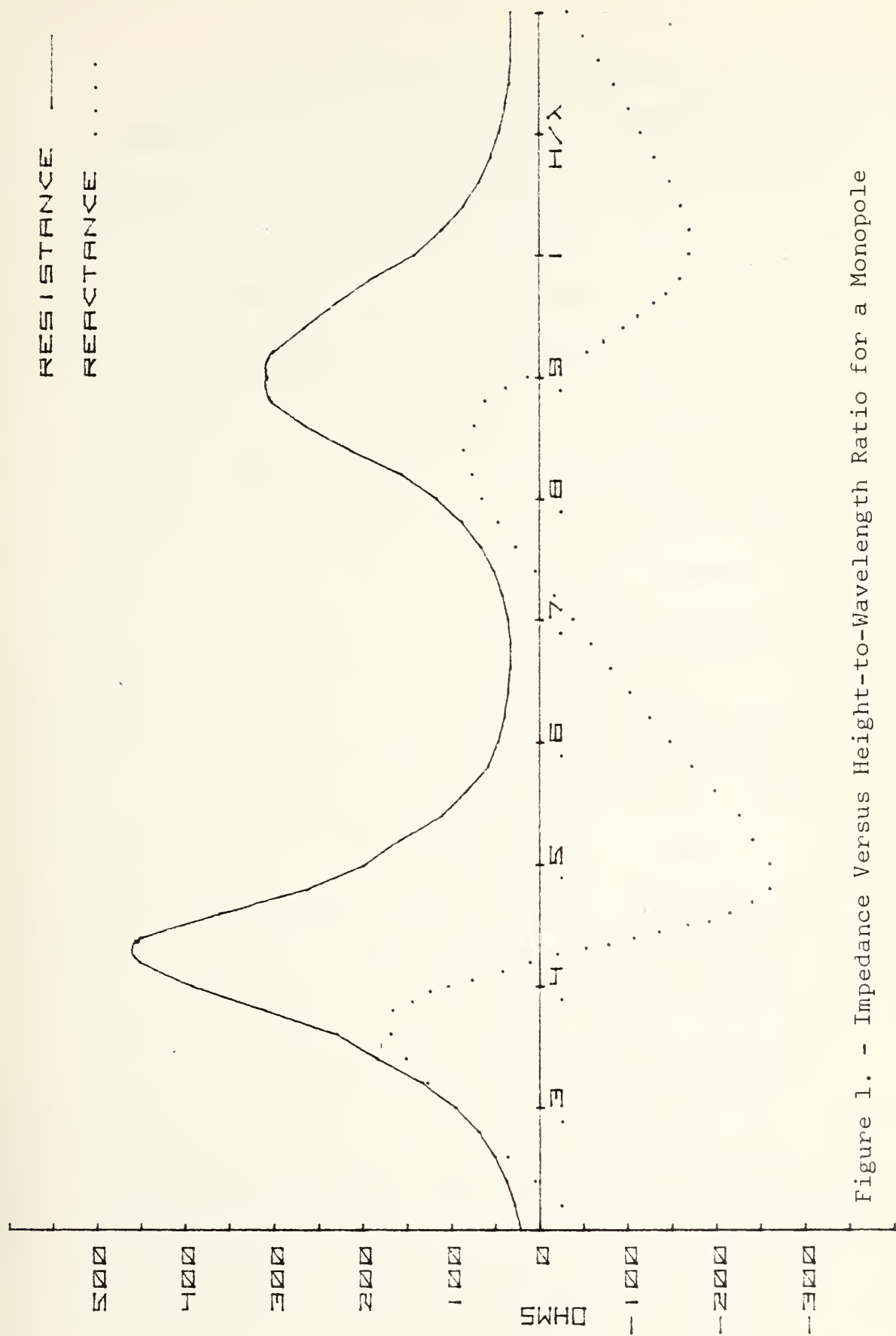


Figure 1. - Impedance Versus Height-to-Wavelength Ratio for a Monopole

The first zero-crossing of the reactance curve occurs at a height-to-wavelength ratio of about one-quarter and corresponds to an antenna operating at resonance. The charge and current distributions for the one-quarter wavelength monopole antenna are shown in Figure 2(a). The next zero-crossing of the reactance curve and the first peak of the resistance curve occur at a height-to-wavelength ratio of about one-half and correspond to an antenna operating at antiresonance. The charge and current distributions for the half wavelength monopole antenna are shown in Figure 2(b). As the height-to-wavelength ratio increases there will be an occurrence of alternating resonance and antiresonance. The resonance corresponding to odd one-quarter height-to-wavelength ratio, and antiresonance corresponding to even one-quarter height-to-wavelength ratio. The charge and current distributions for the three-quarter wavelength monopole antenna are shown in Figure 2(c), and the distributions for a full wavelength monopole are shown in Figure 2(d).

Due to end-effect and shortening of the wavelength on the antenna when compared to the freespace wavelength, the resonance and antiresonance will not occur at exact

multiples of one-quarter height-to-wavelength ratio but will occur at a lower frequency. The height of the peaks of the resistance and reactance curves are related to the height-to-radius ratio. As the ratio increases the peaks will also increase. In the limit as the radius approaches zero the peaks will approach infinity.

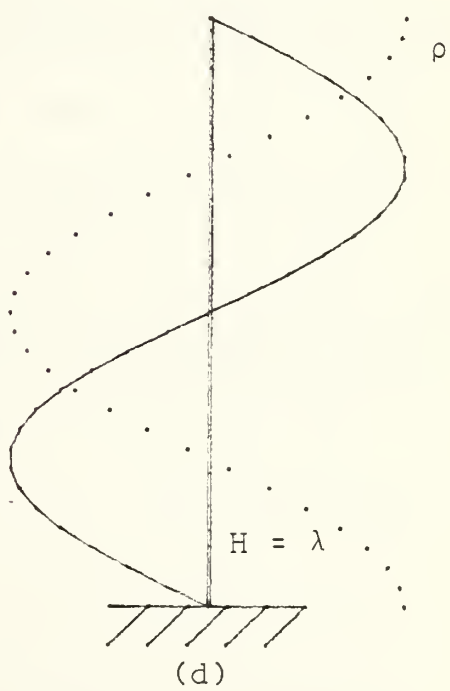
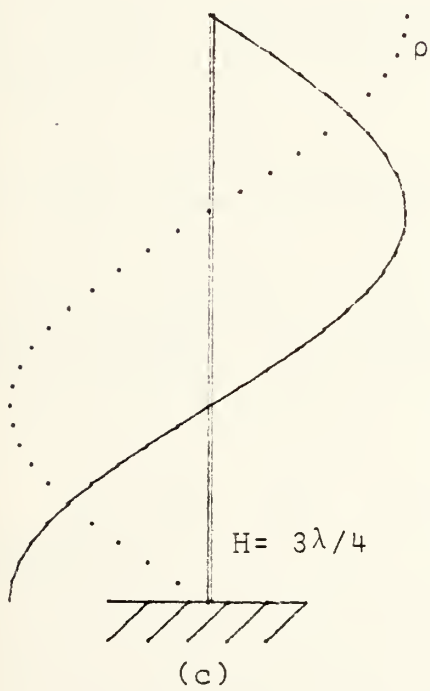
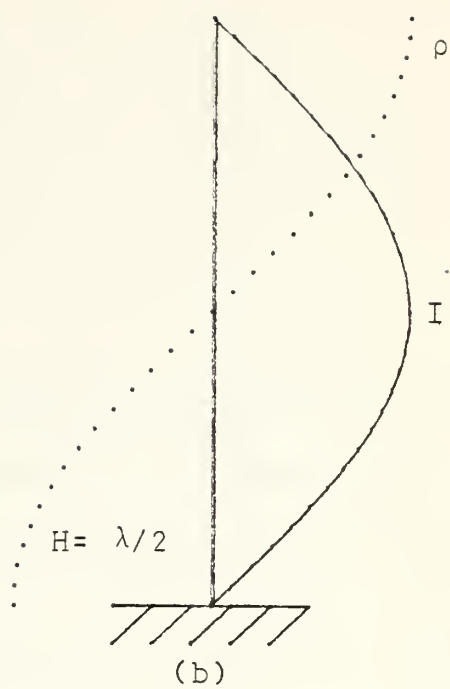
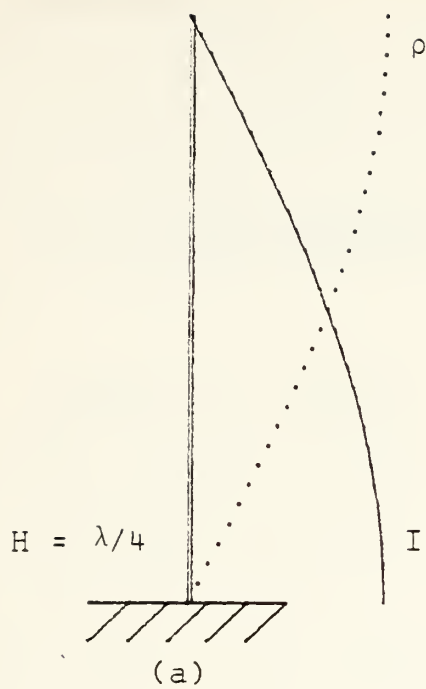


Figure 2. - Monopole Charge and Current Distribution

B. CROSSED-MONOPOLE

1. As a Loaded Monopole

Figure 3 (a) shows a crossed-monopole antenna with the cross placed on top of a monopole of height h_1 . The arms of the cross provide additional conductors on which current can flow and charge can accumulate, and also create a capacitance effect between the loading elements and the image plane. The additional capacitance gives the antenna an effective height which is longer than h_1 . This effect is often used when constructing VLF antennas by placing a top hat on the antenna in order to improve the antenna input characteristics. The increased effective height caused by the arms also increases the height-to-radius ratio which will increase the magnitude of the resistance at antiresonance.

The amount of capacitance and the increase in the effective height is directly related to the length of the

arms. If h_3 and h_4 are the same length then the antiresonant peaks on the plot of resistance versus frequency will remain sharp; but, if h_3 and h_4 are of different lengths, then the antiresonant peaks will be wider or two peaks may occur.

As the arms on the crossed-monopole are lowered, as shown in Figure 3(b), the effective height of the antenna will decrease. The monopole section (h_1) is now shorter and is loaded with three elements (h_2, h_3 , and h_4). In the general case where all three loading elements are of different lengths, the results become extremely complex. There can exist resonance or antiresonance with h_1 and any of the loading elements, and also resonance may take place on any combination of two of the loading elements.

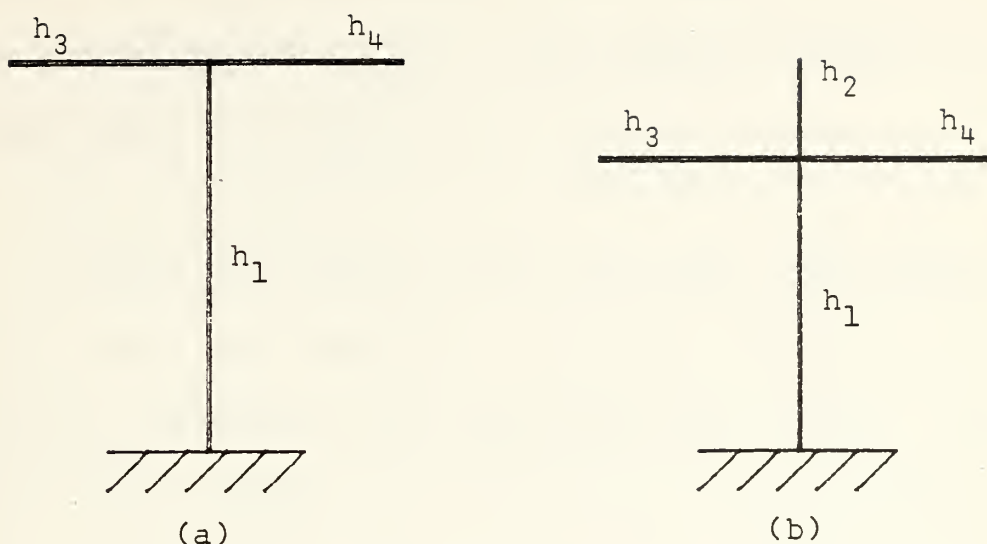


Figure 3. -
Crossed-Monopole Antennas

2. Charge and Current Distribution

The boundary conditions at the junction are equal distribution of the charge between the connecting conductors and Kirchoff's current law which when applied at the junction requires the summation of the currents be zero. Since the arm elements are perpendicular to the monopole, there is no inductive coupling between the monopole and the arm. The electric (E) field emanating from the monopole is oriented radially so as to induce opposing currents in opposite arms. The magnitude of these induced currents and

thus the magnitude of the charge and current distributions on the arms is proportional to the strength of the E field which is directly related to the surface charge in the proposed junction region.

Figure 4(a) shows the zero-order distribution of charge along the vertical conductor when the cross is located at a minimum in the standing-wave pattern. Owing to symmetry the forces in the horizontal arms caused by the charge in the two adjacent quarter wavelength of the standing-wave distribution will be 180 degrees out of phase and provide mutually canceling forces. The only force which will cause current in the arms must come from the charge distribution remotely located from the junction, therefore, the currents on the horizontal arms will be small.

Figure 4(b) shows the zero-order distribution of charge along the vertical conductor when the cross is located at a maximum in the standing-wave pattern. The charge near the junction no longer creates forces in the arms which are 180 degrees out of phase, but exerts forces which are uncanceled in the arms and parallel to the arm axis. These forces act to induce currents in the arms.

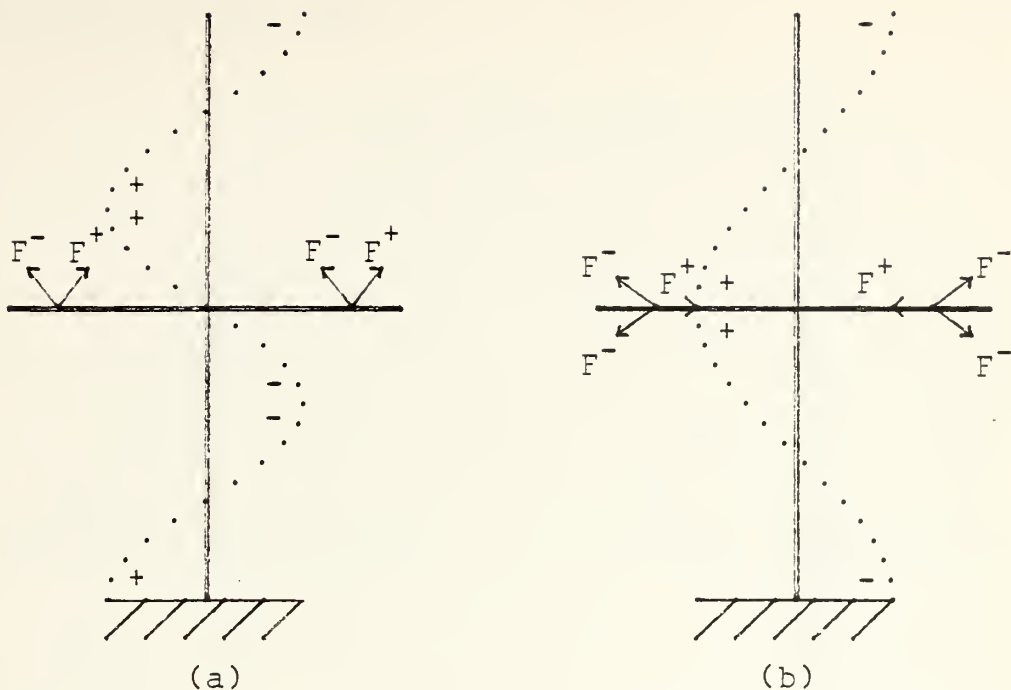


Figure 4. -
Illustration of Forces Acting on Charges
in the Horizontal Elements

Figure 5(a) and 5(b) illustrates the zero-order charge and current distributions of the horizontal arms of one-quarter wavelength and one-half wavelength respectively. In practice the distributions on both the vertical member and horizontal arms will be different from the zero-order distributions shown. The forces between the charges on the different members will modify the distributions. This effect is most noticeable when a charge maximum occurs at the junction. When analyzing the input impedance over a wide range of frequency for various crossed-monopole structures all possible combination of the above

distributions may occur.

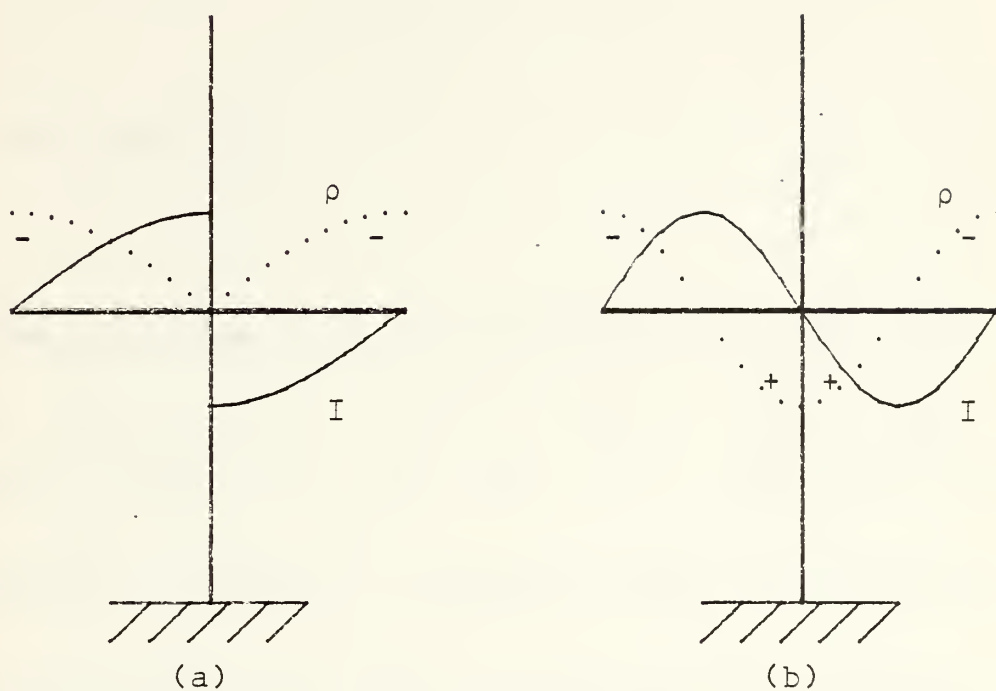


Figure 5. -
Charge and Current Distributions on Quarter
and Half-Wavelength Horizontal Elements

III. EXPERIMENTAL EQUIPMENT

A. WIRE STRUCTURES

The monopoles and crossed-monopoles were constructed using American (B&S) gauge 19 solid copper wire. The nominal diameter of the wire is .91 mm with an ohmic resistance of 1.66×10^{-5} ohms/mm at 20°C. The junctions of the crossed-monopoles were constructed using 3AG60SN solder and then shaped to maintain uniform dimension. Length dimensions were controlled to within ± 0.1 mm.

Figure 6 is a photograph of the wire structures used in this experiment, and Figure 7 is a drawing of the antennas. Note that in some cases in order to obtain a structure with the arm at a different position a previously used structure was merely inverted. Except in cases where the top of the vertical member was removed in order to separate its effect from that of the arms, all vertical members of the

crossed-monopoles are 30 mm. In the frequency range used (2-12GHz) this length corresponds to a length of less than one-quarter wavelength for the lowest frequency to about five-quarters of a wavelength for the highest frequency.

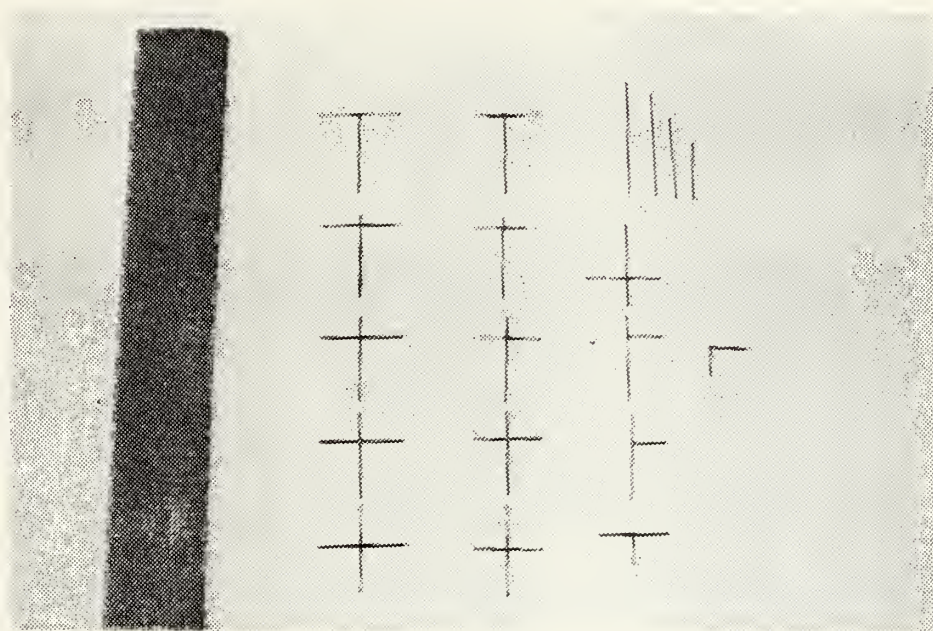


Figure 6. - Photograph of the Wire Structures

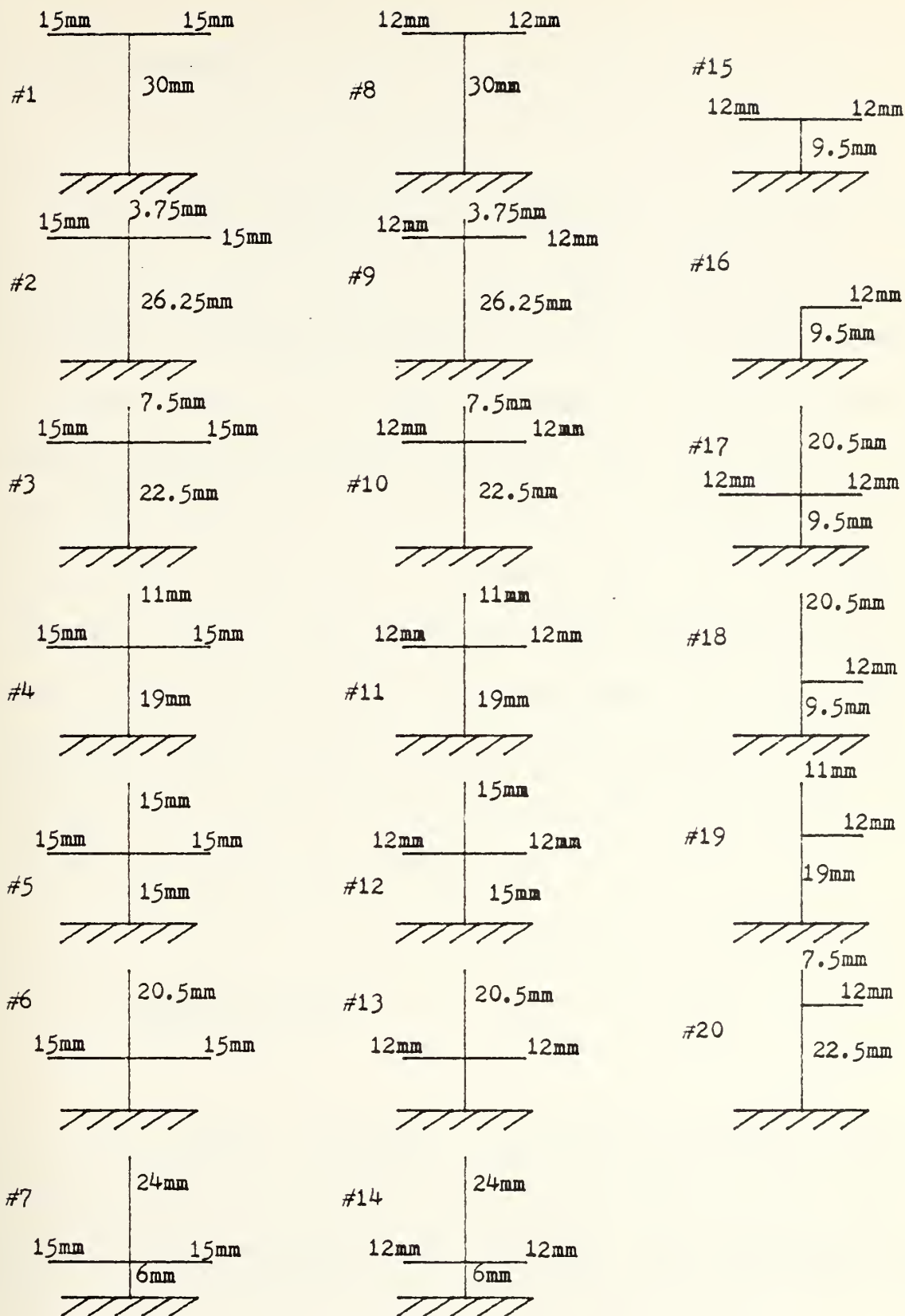


Figure 7. - Antennas

B. TEST FIXTURE

Three major features were considered in choosing the appropriate test fixture. The reflections caused by the connectors and adapter should be minimal in order to reduce the distortion in the impedance curves. To avoid resonant effects between the center conductor and the shield, the space from the center of the adapter to the shield should be small when compared to the wavelength of the highest frequency used. Also the ground plane dimensions should be large when compared to the wavelength of the lowest frequency used in order to minimize the effects of a finite ground plane. Several configurations were tried before the one described below was chosen.

1. Female Adapter

An OSM217 miniature in-series jack/jack coaxial adapter was used in order to connect to the ground plane. Figure 8 is a drawing of the adapter. Note the dimensions comply with the second consideration listed above. A hole

was drilled and tapped in the ground plane and the adapter was screwed into the tapped hole. The flange on the adapter was ground down flush with the center insulator and the adapter adjusted to fit flush with the ground plane. The resulting fixture allowed the wire antennas to be inserted 1.5 mm into the hollow center conductor of the adapter.

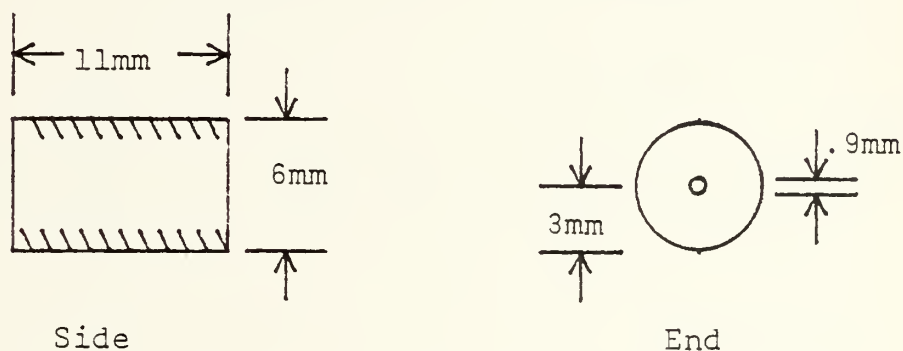


Figure 8. - Female Adapter

2. Ground Plane

The ground plane was constructed from a square, 5 mm thick, plate of aluminum with sides of 61 cm. Note the dimension comply with the third consideration listed above.

In order to minimize the number of interfaces in the electrical connection between the test fixture and measuring equipment, the ground plane was mounted vertically in a wooden rack and the adapter connected to the measuring equipment with a single connector. Figure 9 is a drawing of the ground plane showing the position of the adapter. Figure 10 is a photograph of the ground plane with an antenna mounted in the adapter.

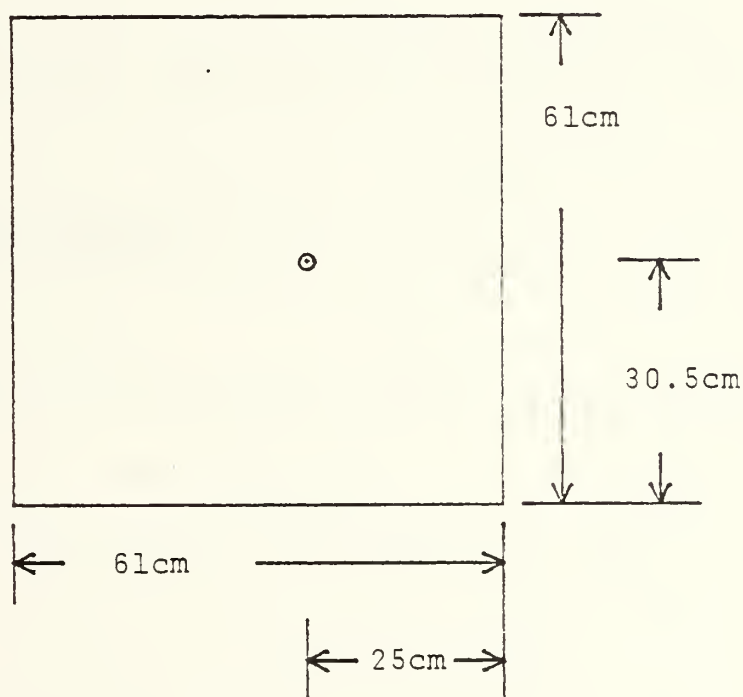


Figure 9. - Ground Plane

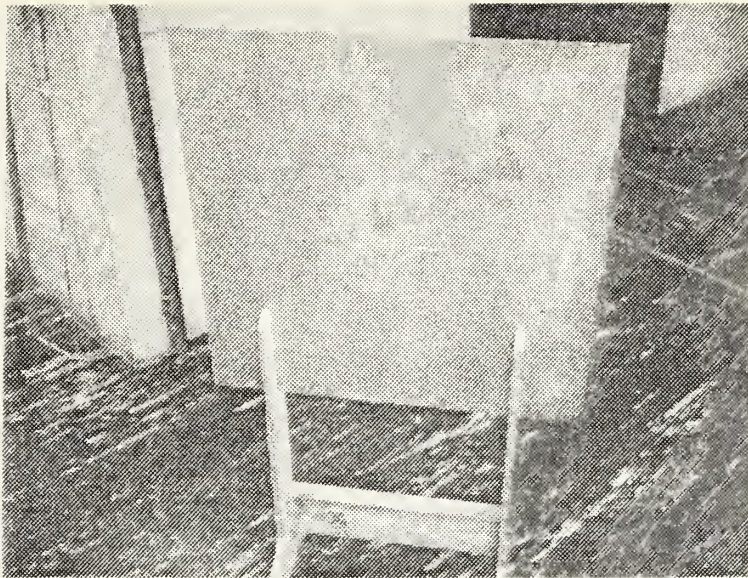


Figure 10. - Photograph of the Ground Plane

3. Anechoic Chamber

In order to minimize the return of radiated energy, the test fixture was immersed in an anechoic chamber. Figure 11 is a photograph of the anechoic chamber with the wooden rack used to hold the ground plane in position. The chamber was constructed using 10 cm thick Eccosorb H radar absorbing material and had dimension of 120 x 60 x 60 cm. One side of the chamber was open so that the chamber could be pushed over the vertically mounted ground plane. In order to check the effectiveness of the chamber, the readout

of the measuring equipment was observed while the chamber was placed over the ground plane and removed. Also while the chamber's position was shifted. Interference from returned energy was observed in the 2-4 GHz range with the chamber removed. No effects from returned energy were observed with the chamber in place.

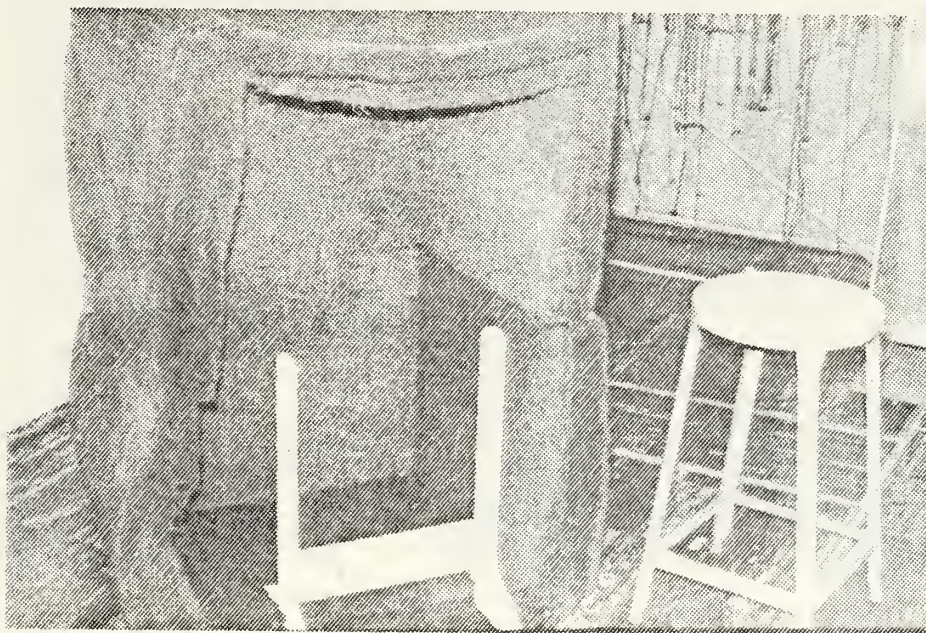


Figure 11. - Photograph of the Anechoic Chamber

C. MEASUREMENT SYSTEM

1. Configuration

Impedance measurements were made using the HP-8410s Microwave Network Analyzer and Wang 600 Programmable Calculator. The results of the measurements were impedance data in tabulated form. Figure 12 is a photograph and Figure 13 is a block diagram of the Network Analyzer.



Figure 12. - Photograph of the Network Analyzer

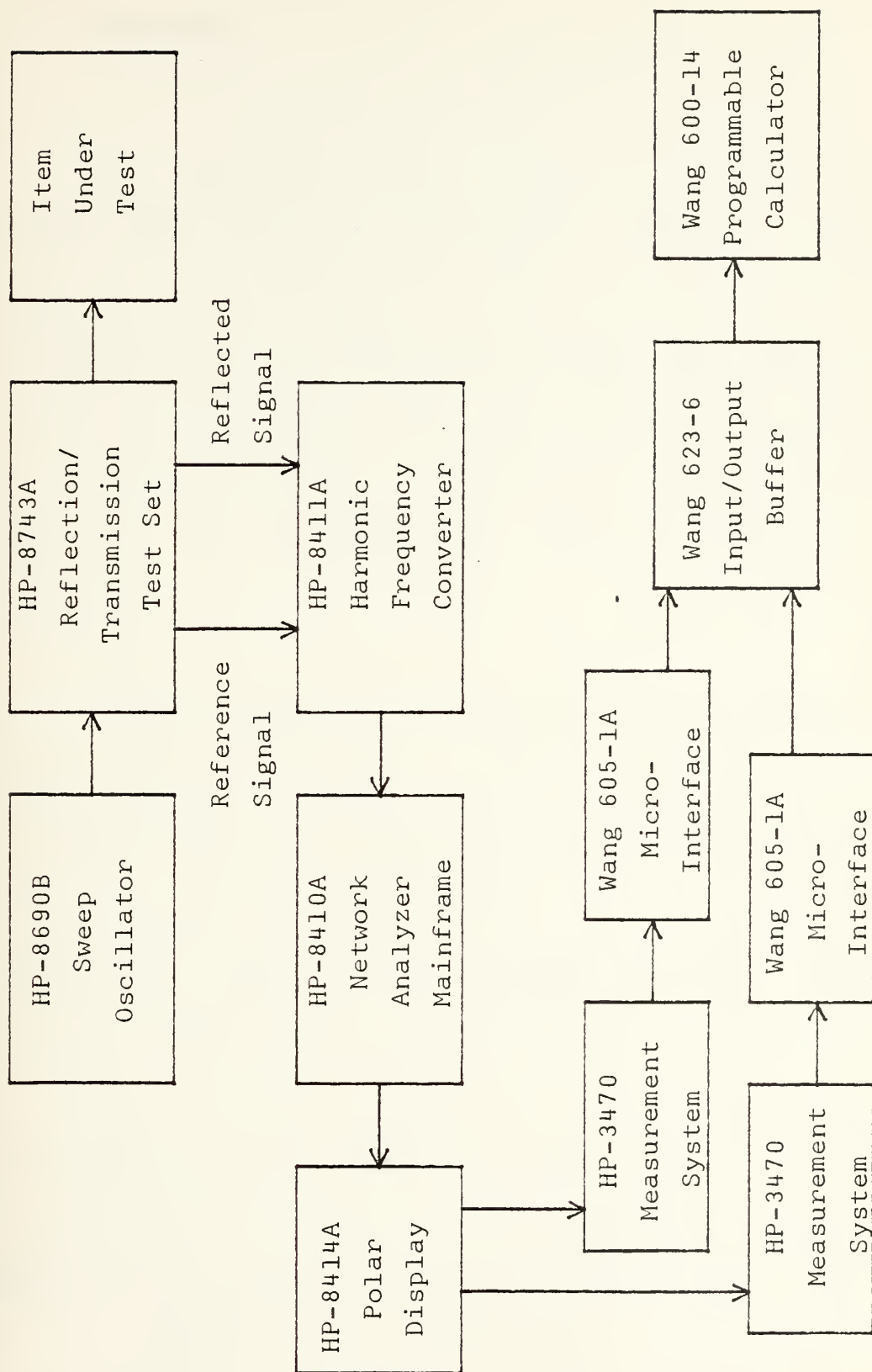


Figure 13. - Block Diagram of the Network Analyzer

2. Operation

By utilizing three different RF units in the HP-8690B Sweep Oscillator the desired frequency range was covered in three steps (2-4 GHz, 4-8 GHz, and 8-12 GHz). The output of the oscillator was feed into the HP-8743A Reflection/Transmission Test Set where a reference signal was coupled off and sent to the HP-8411A Harmonic Frequency Converter. The remaining RF signal was sent to the item under test.

When the test item's input impedance differed from the characteristic impedance of the transmission line, part of the RF signal was reflected back into the test set. The reflected signal was coupled into the harmonic frequency converter by use of a directional coupler. Both the reference signal and the reflected signal were sampled in the harmonic frequency converter, and the samples were sent to the HP-8410A Network Analyzer Mainframe. By comparing the amplitude and phase of the reflected and reference samples in the network analyzer the reflection coefficient (k) was determined and displayed on the HP-8414A Polar

Display. The normalized input impedance (z) of the item under test was calculated from the reflection coefficient using the equation shown below.

$$z = (1+k)/(1-k)$$

The normalized impedance was calculated automatically by taking the X and Y voltages from the polar display, which are proportional to the real and imaginary components of the reflection coefficient, and feeding them into a HP-3420 measurement system where the voltages were converted into digital signals. The resulting digital signals were sent through the Wang 635-1A Micro-Interface and the Wang 623-6 Input/Output Buffer into the Wang 600-14 Calculator. The calculator was programmed to use the input digital signals to calculate the normalized impedance and store the information in memory. The normalized impedance was obtained for each desired frequency in the frequency range of interest. The list of the normalized impedances in the calculators memory was printed upon demand.

3. Calibration

In order to obtain accurate data from the network

analyzer the system must first be calibrated using a known load. Normal procedure is to place a short at the plane where the test item is to be placed. This procedure results in a reflection coefficient of magnitude one and phase angle of -180 degrees. The system is then adjusted to give the proper results on the polar display.

Another method of calibrating the system is to use an open at the plane where the test item is to be placed. This procedure results in a reflection coefficient of magnitude one and phase angle of zero degrees. Since an open coaxial line is not of infinite impedance but has some small value of capacitance, some error will result from this procedure. However, as shown below, the error resulting from the use of an open for calibration was small when compared to the improvement in the resulting impedance plots.

In order to get an accurate impedance versus frequency plot, a large number of points was desirable. Due to nonlinearities in the system the system required calibration for each frequency used, and it became impractical to use the procedure described above. Instead the impedance of both the open test fixture and the antenna

under test were measured at each desired frequency and the value of the impedance for the open test fixture was used to correct the measured impedance of the test antenna. This method of correction had the same effect as calibrating the system for each frequency.

Figure 14, Figure 15, and Figure 16 are plots of the measured magnitude and phase of the reflection coefficient versus frequency for the open test fixture, 30 mm monopole, and 39 mm monopole respectively. The reflection coefficient for the open test fixture should have a magnitude of one with a phase of zero degrees. The distortions in the reflection coefficient are caused by reflections from the interfaces of the numerous connectors in the system.

In order to determine the effects of the connector required to connect the test fixture to the measurement equipment, a short was placed directly on the measuring equipment, and similar distortions in the measured reflection coefficient were noted. The distortions in the reflection coefficient for the open test fixture were of the same magnitude as those for a short placed directly on the measuring equipment, therefore, the additional connector required to connect the test equipment added little to the

overall errors in the system.

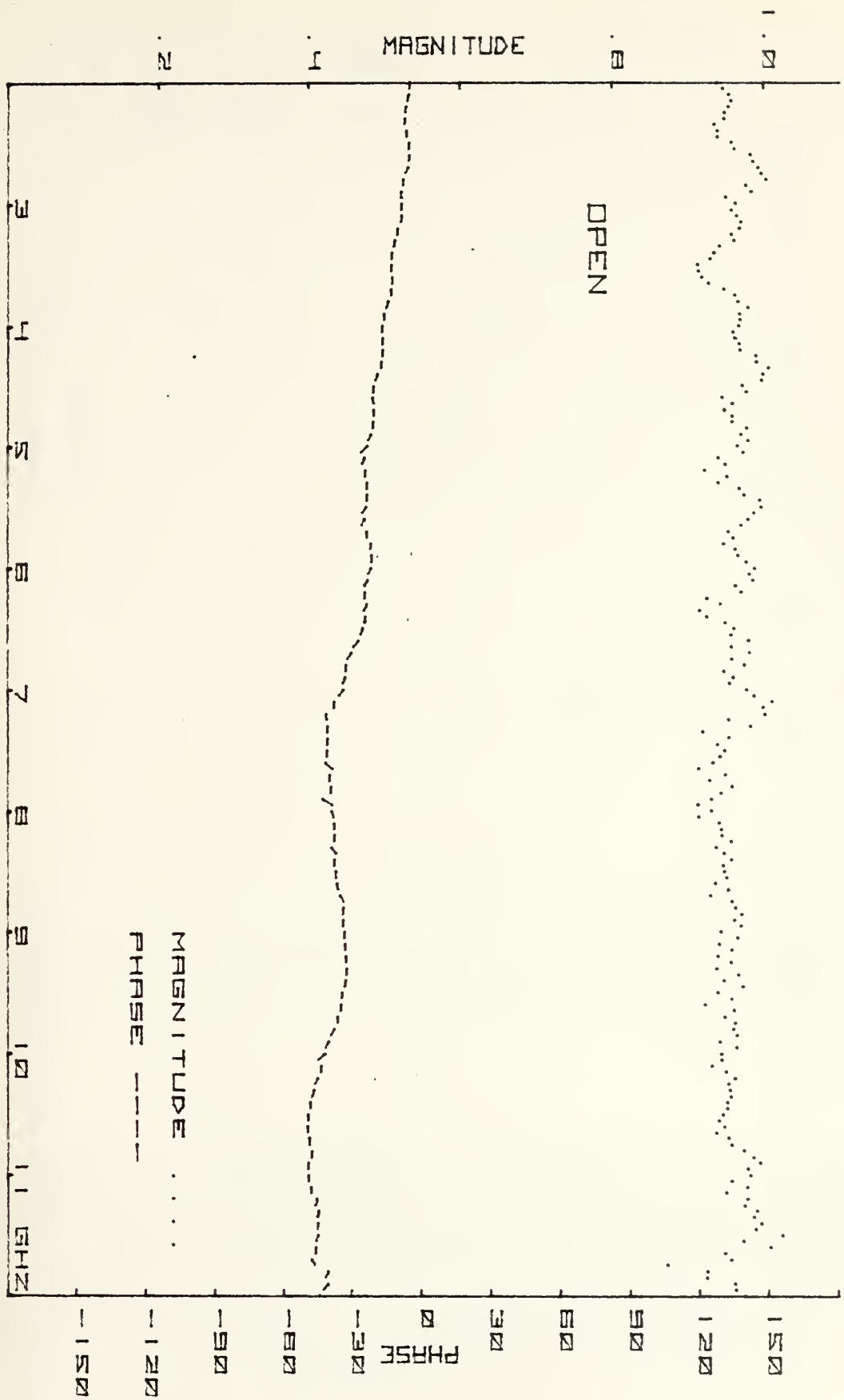


Figure 14. - Reflection Coefficient Versus Frequency
for the Open Test Fixture

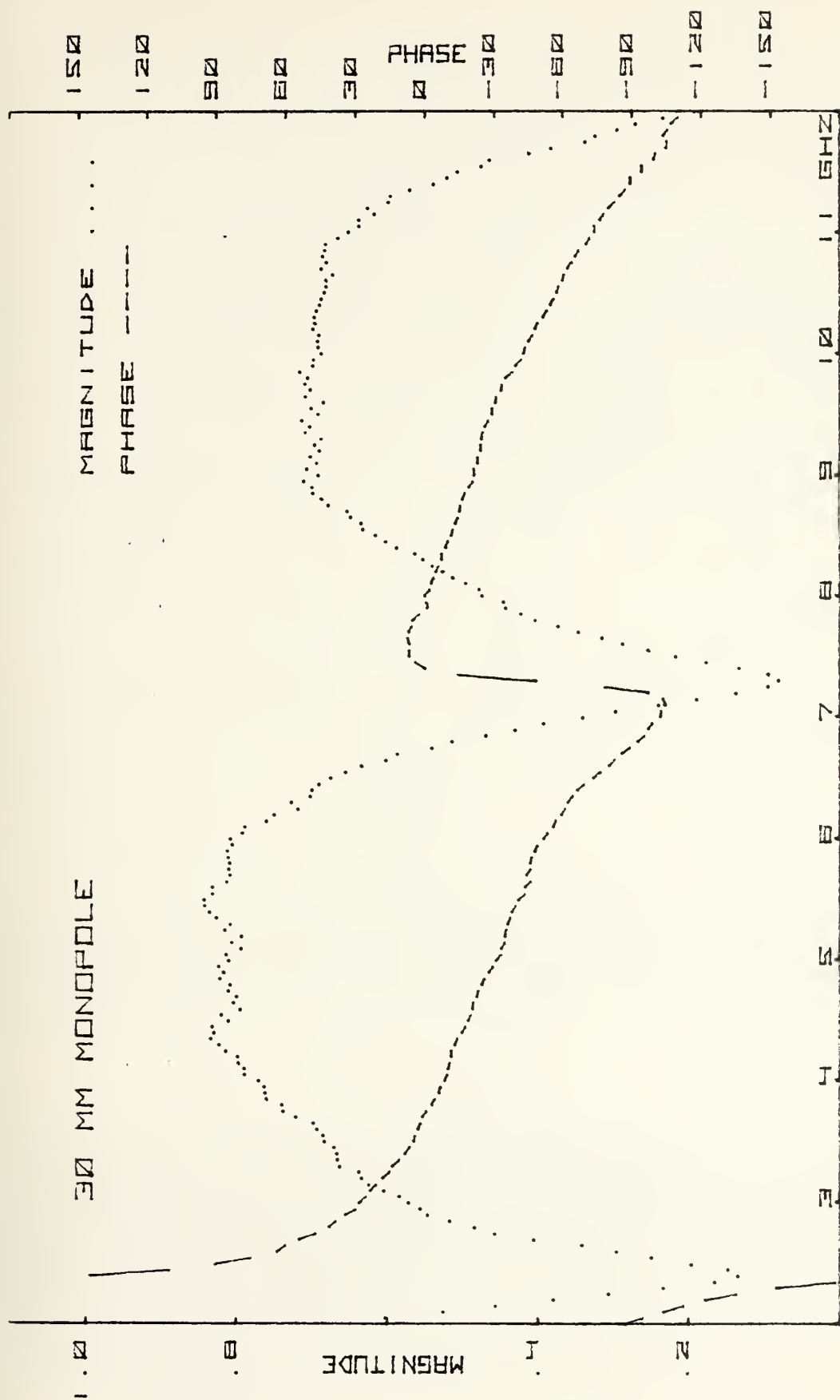


Figure 15. - Reflection Coefficient Versus Frequency
for the Uncorrected 30 mm Monopole



Figure 16. - Reflection Coefficient Versus Frequency
for the Uncorrected 39 mm Monopole

In Figure 15 and 16 the peaks in the magnitude curves correspond to antiresonance, and the dips to resonance. The curves are smooth during resonance, but there are distortions in the curves caused by reflections from the connector interfaces during the antiresonance. During antiresonance the antenna's reflection coefficient is similar to that of an open. The effects of the connector interfaces in this area is also similar to that of an open, therefore, the use of an open to correct the measurements of the antenna canceled much of the effects of the connector interfaces. This improvement in the accuracy of the reflection coefficient is the reason the system was calibrated using an open rather than a short.

The equations shown below were used to correct the measured reflection coefficient of the test antennas.

$$k_c = k - k(k_o - 1)$$

$$p_c = p - p_o + p_{o2}$$

k_o = the reflection coefficient magnitude for the open
test fixture

p_o = the reflection coefficient phase for the open test
fixture

p_{o2} = the reflection coefficient phase for the open test
fixture at 2 GHz

k = the reflection coefficient magnitude of the test
antenna

p = the reflection coefficient phase of the test antenna

k_c = the corrected value for the reflection coefficient
magnitude of the test antenna

p_c = the corrected value for the reflection coefficient
phase of the test antenna

By first calibrating the system on a short, the distortions in k_o varied about one. Subtracting one from k_o gave the measured value of the error. From Figure 15 and 16 it was observed that the distortion in k increased as k increased. As shown in the equation above, a linear relation was assumed and gave good results. The measured value of the distortion multiplied by k was subtracted from k to obtain the corrected value for the magnitude of the reflection coefficient.

The phase for an ideal open should be zero, but due to nonlinearities and the distortions the measured value of p_o was not zero. The nonlinearities caused a phase shift which was a function of frequency, and the distortions were a function of frequency and also of the magnitude of the reflection coefficient. Since the exact nature of the phase shift caused by nonlinearities was unknown, the two effects could not be separated. Subtracting p_o from p did not account for changes in p_o as a function of k but gave good results. In order to correct for the error caused by calibrating the system on an open, p_{o2} was added to $p - p_o$. This procedure is not exact since the error is a function of frequency, but it did add to the overall accuracy of the results. Figure 17 is a plot of the reflection coefficient for the 30 mm monopole after the measurements have been corrected using the measurements taken of the open test fixture. Although not all of the distortions have been canceled, considerable improvement was obtained.

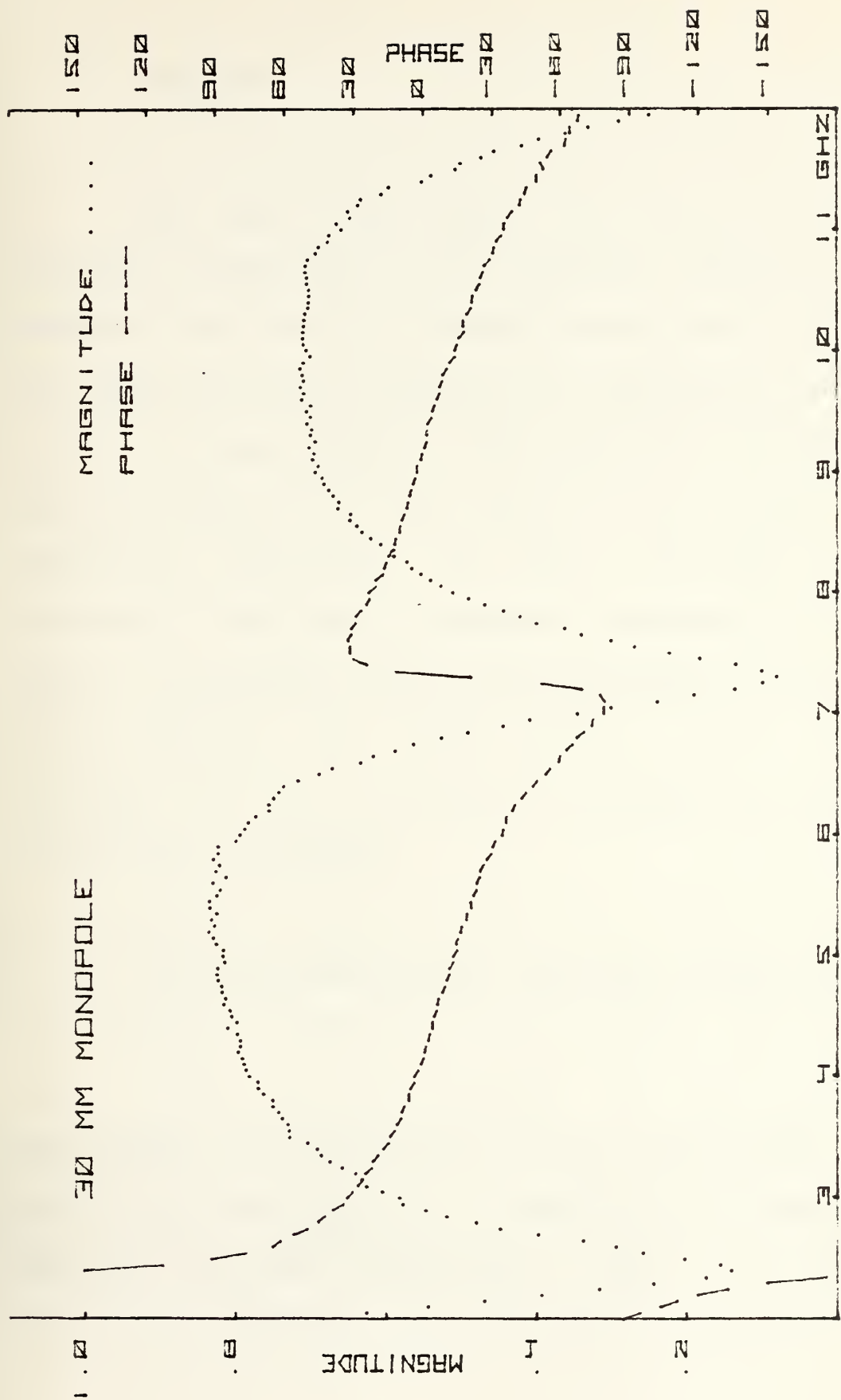


Figure 17. - Reflection Coefficient Versus Frequency
for the Corrected 30 mm Monopole

4. Accuracy

The Smith Chart shows the relation between the reflection coefficient and the normalized impedance. It is observed that when the reflection coefficient is large with zero phase then small changes in the reflection coefficient result in large changes in the normalized impedance. From observing Figure 17 it is estimated that errors in the reflection coefficient of about $\pm 3\%$ exist when the reflection coefficient's magnitude approaches one. This error is considered within the limitations of the equipment used. However, the percent error in the calculated impedance may be larger due to conversion from reflection coefficient to impedance.

It is unfortunate that the largest errors occur when the reflection coefficient is large thereby increasing the error in the calculated impedance. But this results is as anticipated. As mentioned earlier the distortions in the reflection coefficient are caused by reflections from the numerous connector interfaces. When the reflection coefficient magnitude is small most of the power from the

source is being radiated by the antenna and only small errors are noted, but when the reflection coefficient magnitude is large then the energy is reflected back into the source, and additional distortion is caused by the connector interfaces due to the two-way travel and resonant effects set up between interfaces.

IV. EXPERIMENTAL PROCEDURE

A. DATA ACQUISITION

Data was acquired using the equipment described in section III. Each time the test fixture was setup the following procedure was used. First the network analyzer was calibrated at 2 GHz using a short placed at the same physical distance from the test set as the ground plane. Next, with the open ground plane attached, impedance measurements were taken every 50 MHz from 2 to 12 GHz. Since the measurements taken of the open ground plane were used to correct the antenna measurements, the open ground plane measurements were taken every time the system was setup in order to minimize the effects caused by changes in the setup or calibration. Measurements were then taken of the desired antennas. The measurements were again taken at every 50 MHz from 2 to 12 GHz with frequency accuracy held to ± 1 MHz.

B. DATA PROCESSING

The data acquired as stated above was a printed list of the normalized impedance for each frequency step. The data was entered into the HP 9821A calculator where it was corrected using the equation described in section III and then plotted on the HP 9862A plotter. Figure 18 is a photograph of the HP 9821A calculator and HP 9862A plotter.

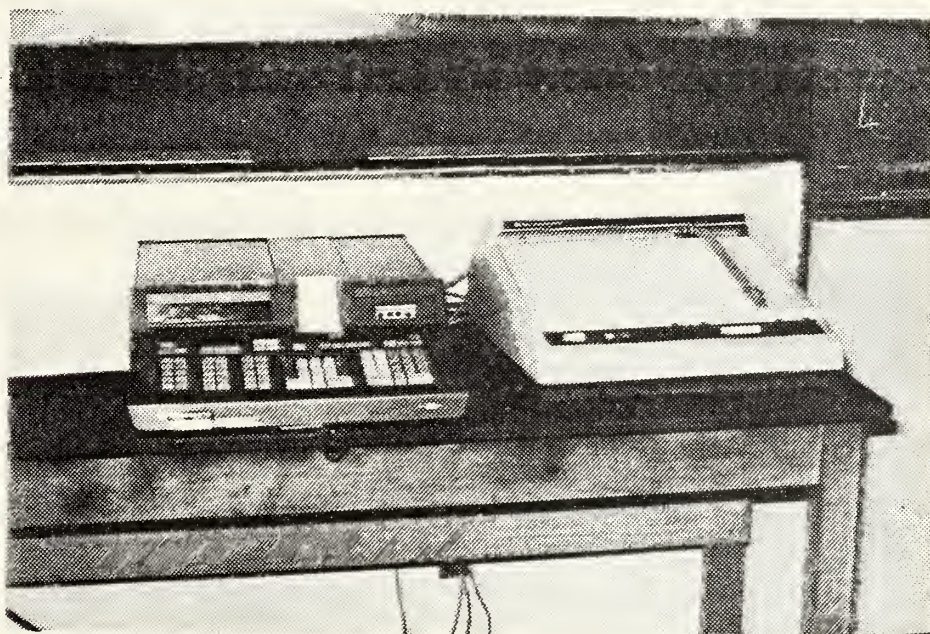


Figure 18. - Photograph of the HP 9821A Calculator
and HP 9862A Plotter

C. ACCURACY

Figure 19 is a plot of the measured impedance versus frequency for a 30 mm monopole compared to theory. The information for the theoretical monopole [Jordan and Balmain 1968] is for a 30 mm monopole with a height-to-radius ratio of about 60. The test monopole also has a height of 30 mm and a height-to-radius ratio of about 67.

Note the distortions in the peaks of the measured curves. These distortions are caused from errors in the measured reflection coefficient. When the reflection coefficient is large with zero phase the resulting error in the calculated impedance is large. These condition occur on the impedance plots when the magnitude of the resistance is large and the reactance is changing from positive to negative. Figure 20 is a polar plot of the reflection coefficient on a Smith Chart. It can be clearly seen on Figure 20 that in the areas of 4-5 GHz and 9-10 GHz a small change in the reflection coefficient will cause a large change in the impedance.

There is also a horizontal shift at 9 GHz in the measured curves when compared to the theoretical. The source of this error is probably the result of the method

used to calibrate the system. When a voltage is applied to an open coaxial line the electric field will bulge outward. This bulging has the effect of extending the plane of reflection, therefore, the system was calibrated to a plane slightly beyond the end of the coaxial line. The change in the phase of the reflection coefficient with a short and with an open was measured at 2 GHz, and this value was used to compensate for the error caused by calibrating the system on an open. However, the error is somewhat frequency dependent, therefore, some error is still observable. This error is small and does not detract from the overall shape of the impedance curves.

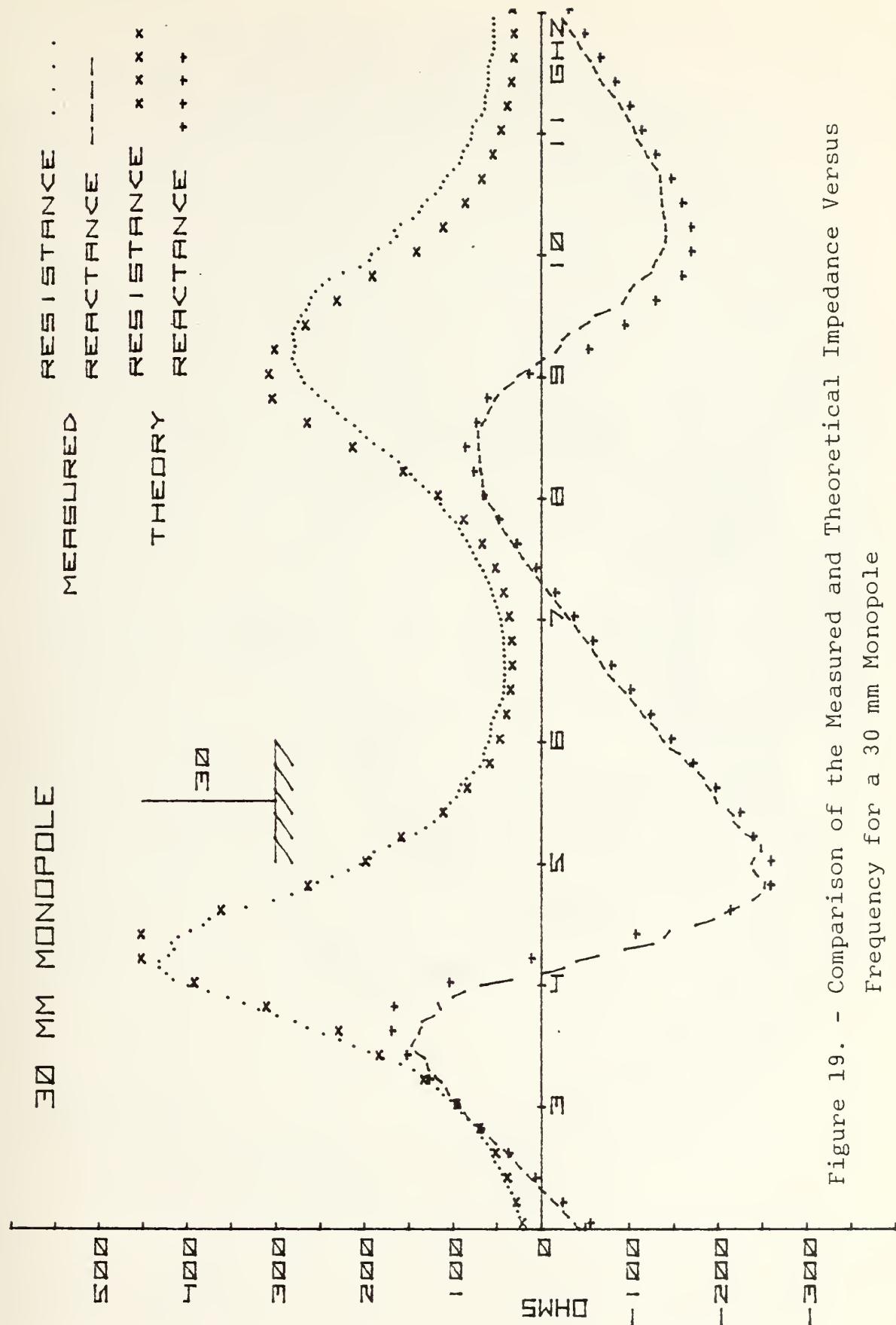


Figure 19. - Comparison of the Measured and Theoretical Impedance Versus Frequency for a 30 mm Monopole

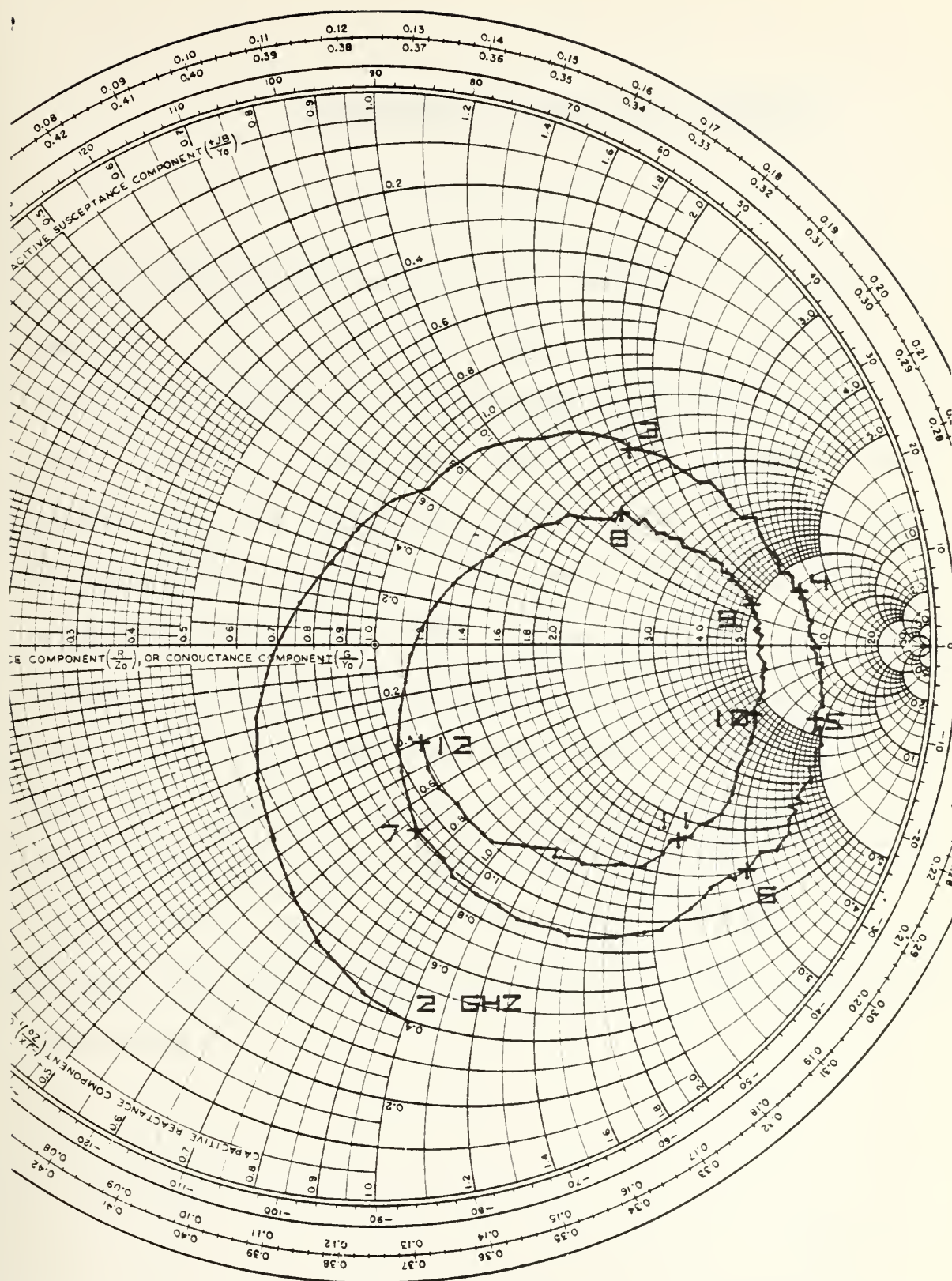


Figure 20. - Polar Plot of the Reflection Coefficient Versus Frequency on a Smith Chart for a Corrected 30mm Monopole

V. EXPERIMENTAL RESULTS AND ANALYSIS

Following are a few general comments concerning the impedance plots which are shown in this section. The frequency is labeled on the horizontal axis and in all plots ranges from 2 to 12 GHz. The vertical axis is labeled ohms, and the scale may differ from plot to plot. The dimension of the antenna figures shown on the graphs are given in millimeters and have been rounded off to the nearest integer. The exact measurements of the antennas can be found in Figure 7. The resistance curves are dotted lines with each dot the result of an experimental measurement. The reactance curves are dashed lines which were created by joining every other pair of data points together. The ends of each dash still are the result of an experimental measurement.

A. MONOPOLES

The impedance characteristics of several monopoles were

measured and the results compared to that of well established theory in order to establish the accuracy and reliability of the measuring equipment and procedures.

1. 21 mm Monopole

Figure 21 is a plot of the measured driving point resistance and reactance for a 21 mm monopole. As noted earlier errors in the measured reflection coefficient cause noticeable distortions of the calculated impedance in the vicinity of resistance peaks.

The quarter-wave resonant occurs at about 3.3 GHz. This value compares well with a theoretical monopole of the same dimensions. The height-to-radius ratio is 46.7, and with some interpolation the theoretical value of the resistance at the half-wave antiresonant peak should be about 410 ohms. This value agrees with the measured value, and the overall shape of the curves agrees with the theoretical curves.

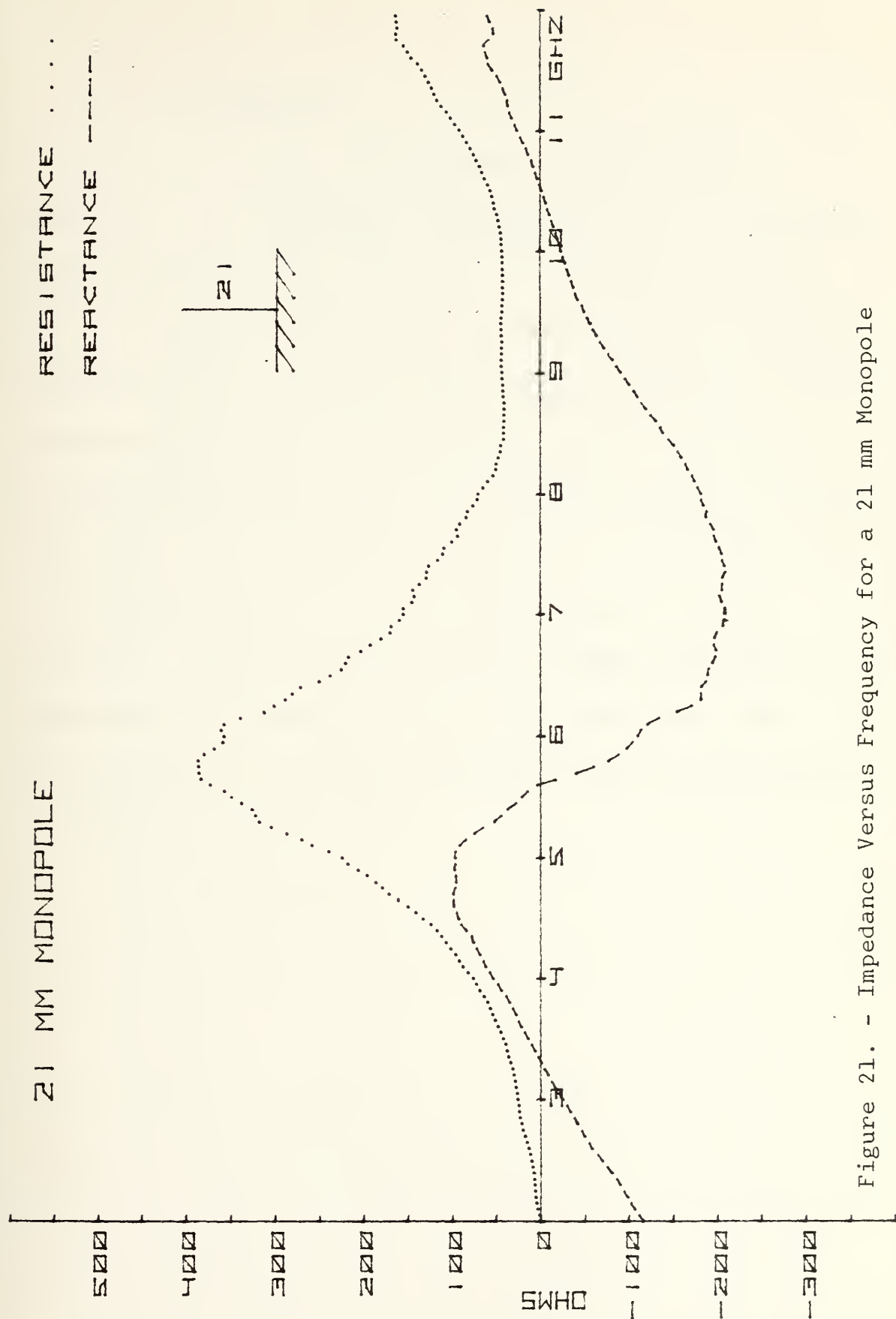


Figure 21. - Impedance Versus Frequency for a 21 mm Monopole

2. 30 mm Monopole

Figure 22 is a plot of the input impedance for a 30 mm monopole. A graphical comparison with a theoretical monopole of the same dimensions was conducted in Figure 19, and a detailed description of the comparison is given in section IV. In comparing the 30 mm monopole impedance characteristic curves with those for the 21 mm monopole, one can easlily see the shift in the half-wave antiresonant point and an occurance of a full-wave antiresonant point. This shift is due to the additional height of the 30 mm monopole. With a longer antenna a longer wavelength, lower frequency, is required to excite the same mode. Also there is an increase in the peak resistance due to the increase in the height-to-radius ratio.

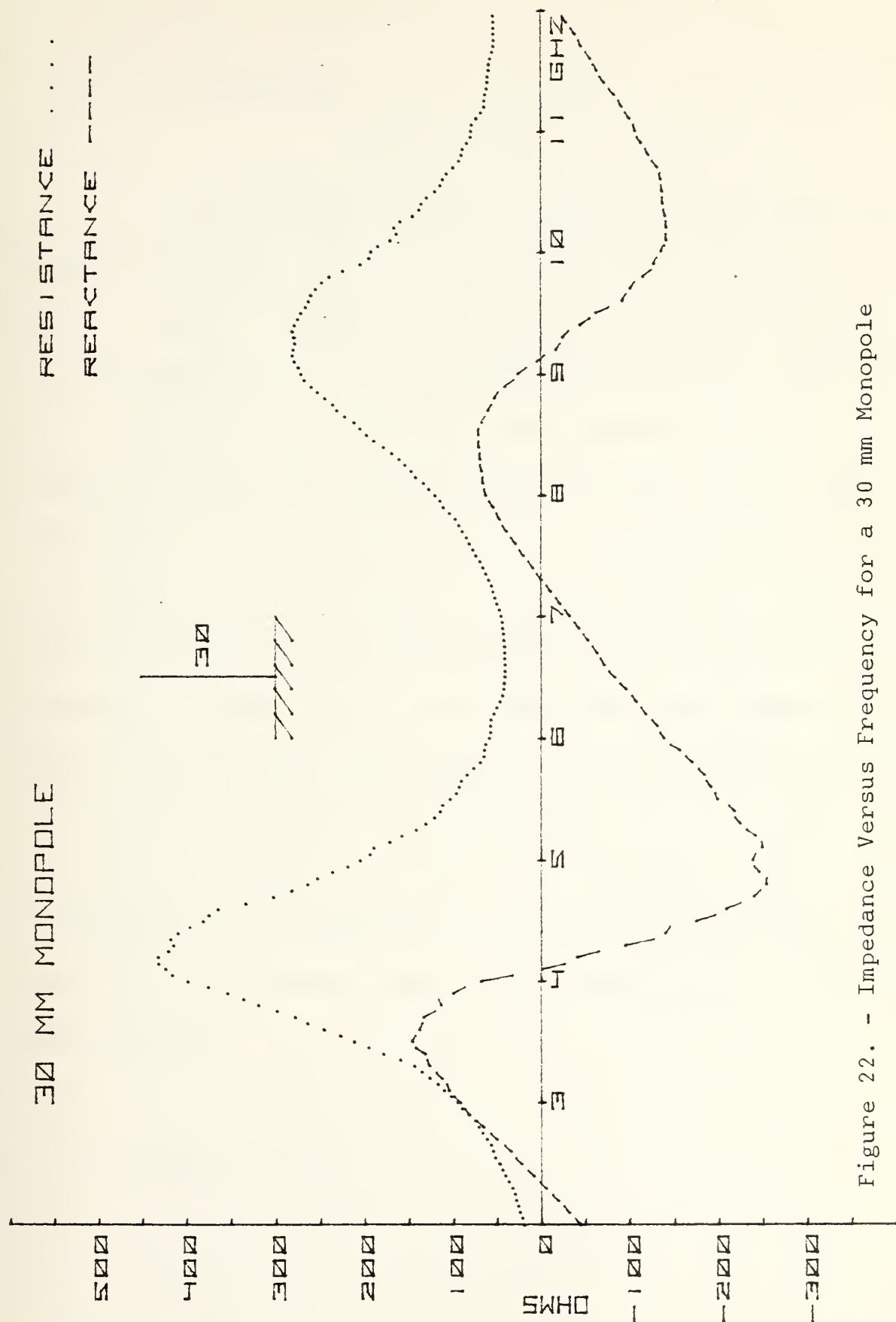


Figure 22. - Impedance Versus Frequency for a 30 mm Monopole

3. 39 mm Monopole

As the height of the antenna is increased the antiresonant peaks shift to the left and the height of the peaks increase. Figure 23 is a plot of the input impedance versus frequency for a 39 mm monopole. The left shift in the half-wave and full-wave antiresonant points, when compared to the 30 mm monopole, can be clearly seen. Also a resistance peak corresponding to a one-and-a-half-wave antiresonant point is visible. The frequencies at which the resonant and antiresonant points occur compare well with the theoretical values. The errors are of the same magnitude as those noted on the 30 mm monopole curves and occur for the same reason. The height-to-radius ratio is 87. From the theoretical graphs [Jordan and Balmain 1968] this corresponds to a resistance of about 580 ohms on the half-wave antiresonant peak which compares well with the measured value.

4. 48 mm Monopole

Figure 24 is a plot of the impedance versus frequency for a 48 mm monopole. Several resistance peaks corresponding to antiresonant effects can be seen. A comparison of the curves with theoretical values gives similar results as the other monopoles.

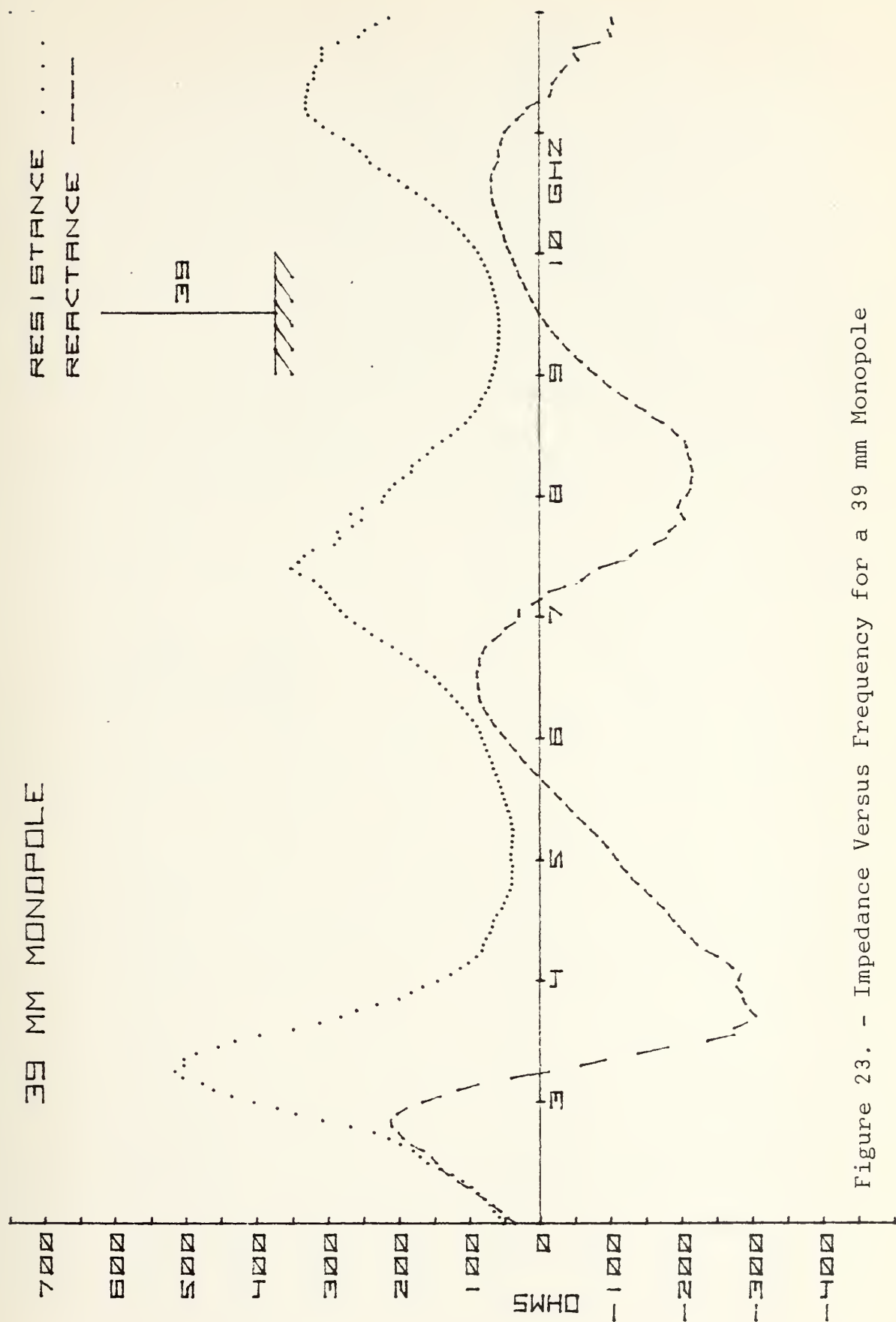


Figure 23. - Impedance Versus Frequency for a 39 mm Monopole

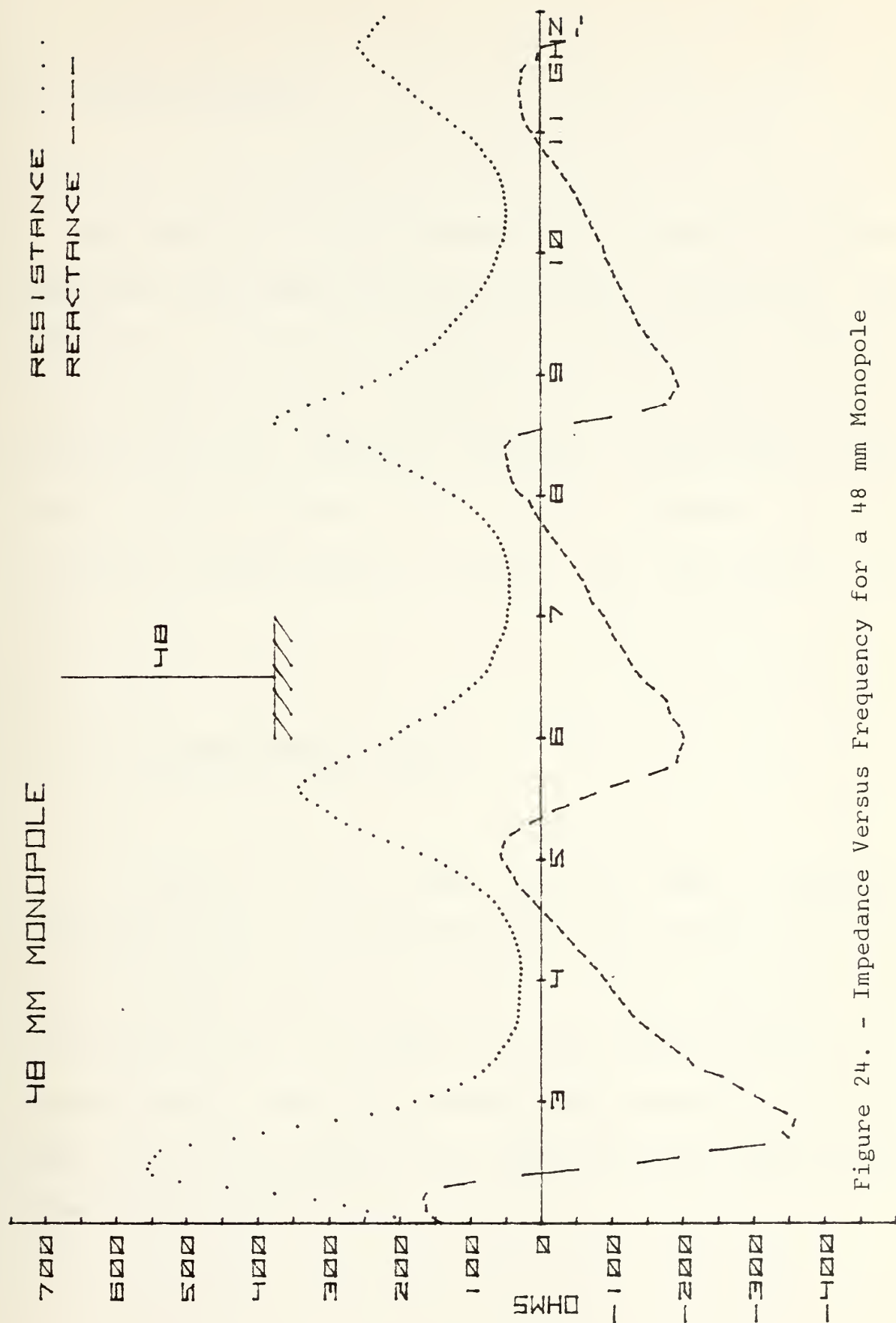


Figure 24. - Impedance Versus Frequency for a 48 mm Monopole

B. CROSSED-MONOPOLE

The results of the measurements on the monopole antennas described above demonstrated the accuracy, reliability, and limitations of the test equipment and procedures. The most noted errors are the distortions of the peaks due to reflections from connector interfaces. These errors limit some of the conclusions that can be obtained from the following crossed-monopole curves, but the effects are small.

1. Crossed-Monopole Case 1

Figure 25 is a plot of the input impedance characteristics of a crossed-monopole Case 1 where two 15 mm arms have been placed on top of a 30 mm monopole. As anticipated from the theory of top loaded antennas, the curves resemble those of a monopole but shifted to the left. This shift to the left has the effect of making the antenna appear taller than 30 mm.

The effective height, from an impedance point of view, of the antenna varies with frequency. At the half-wave antiresonant point, the antenna resembles a 45 mm monopole, and at 5.4 GHz or the three-quarter wavelength resonant point, the antenna appears as a 41 mm monopole. Also for the full-wave antiresonant frequency the antenna resembles a 39.5 mm monopole. This apparent shortening of the antenna as frequency increases is due to a change in the capacitance from the arms to the image plane caused by the change in the charge distribution on the arms.

Figure 5(a) shows the first-order distribution of the charge and current on the arm at one-quarter wavelength. At 2 GHz the 15 mm arm is about .1 wavelengths long, and the charge distribution will be nearly uniform. At about 4.2 GHz the charge distribution will be as shown in Figure 5(a), and there will be less total charge on the arm which will result in less capacitance from the arms to the ground plane. As the frequency increases the total charge will decrease since the additional charge will be of opposite polarity. Figure 5(b) shows the first-order charge and current distributions on the arm when the arm is one-half wavelength long. The negative portion of the charge curve is an excess of electrons, and the positive portion is

exposed positive ions. The capacitance from the arms to the ground plane is distributed over the length of the arms, and due to the change in the charge polarity the sum of the distributed capacitance will be zero. The half-wave distribution should occur at about 9.2 GHz, but the distribution requires a charge maximum at the junction. As seen from measured charge and current distributions [Mc Dowell], as the charge maximum builds up at the junction the repelling effect of the charges on the vertical member tends to decrease the build-up. This effect keeps the zero-order half-wave distribution from occurring. The capacitance of the arms decreases as the frequency increases but does not go to zero.

One can model the resonant points of the impedance curves as series resonant circuits and the antiresonant points as parallel resonant circuits. The resonant frequency is inversely proportional to the squareroot of the capacitance. If one assumes that a change in the resonant frequency is caused by a change in the capacitance, the factor by which the capacitance must change is equal to the square of the ratio of the old resonant frequency over the new resonant frequency. The factor by which the capacitance must increase to change the resonant frequency from that of

a monopole of height equal to the vertical member below the cross to that of the crossed-monopole can be calculated using the above relation. This factor will be an indication of the amount of capacitance added by the arms. Since the model of the input impedance characteristics by alternating series and parallel circuits is not exact, care must be taken when using this analysis technique.

For the Case 1 crossed-monopole, the factors by which the capacitance increases are 2.36 at half-wave antiresonance, 1.86 at three-quarter-wave resonance, and 1.73 at full-wave antiresonance. The effective capacitance decreases as the frequency increases and corresponding to a decrease in the effective height of the antenna. These numbers do not indicate all the changes which take place. The exact equations required to solve for the antenna geometry are extremely complex, but the capacitance factors are useful in comparing different antennas.

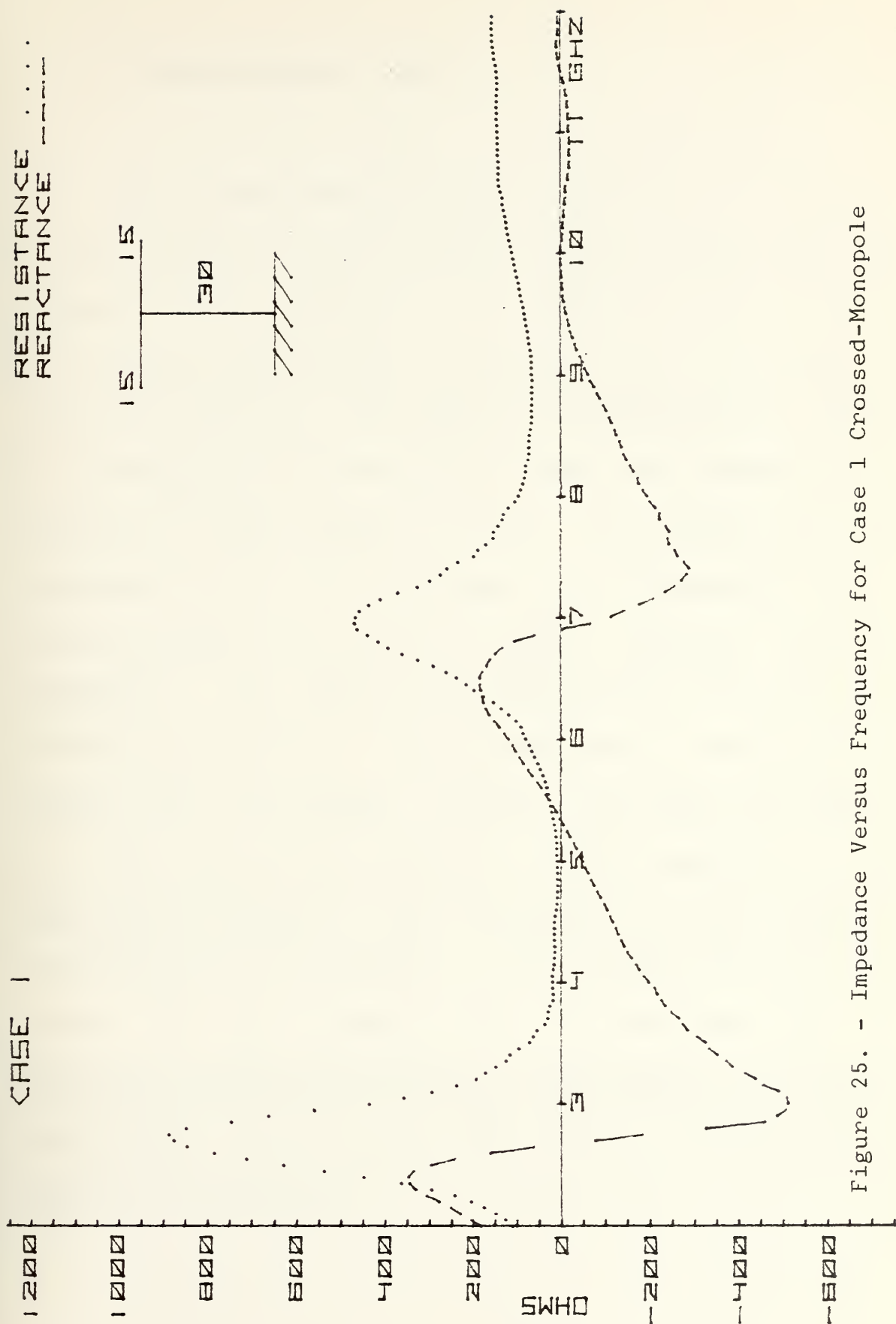


Figure 25. - Impedance Versus Frequency for Case 1 Crossed-Monopole

2. Crossed-Monopole Case 2

The crossed-monopole Case 2 is similar to Case 1, but the arms have been lowered 3.75 mm from the top. The curves are shown in Figure 26. The length of the arms plus the vertical member below the cross for Case 1 is about 1.1 times that for Case 2. For Case 2 the frequencies at which the resonance and antiresonance occurs has increased by a factor of 1.1 when compared to Case 1. The results are as anticipated since the resonance or antiresonance of a shorter antenna will occur at a higher frequency (shorter wavelength). The capacitance factors are 2.57, 2.03, and 1.87 for the half-wave, three-quarter-wave, and full-wave resonant and antiresonant points. The effect of lowering the arms can now be observed in an increase in the capacitance factors. The increase is not directly proportional to the decrease in the height of the arms because of the geometry of the structure, and the capacitance factors are effected by the change in the charge distributions on the arms since they are calculated at different frequencies.

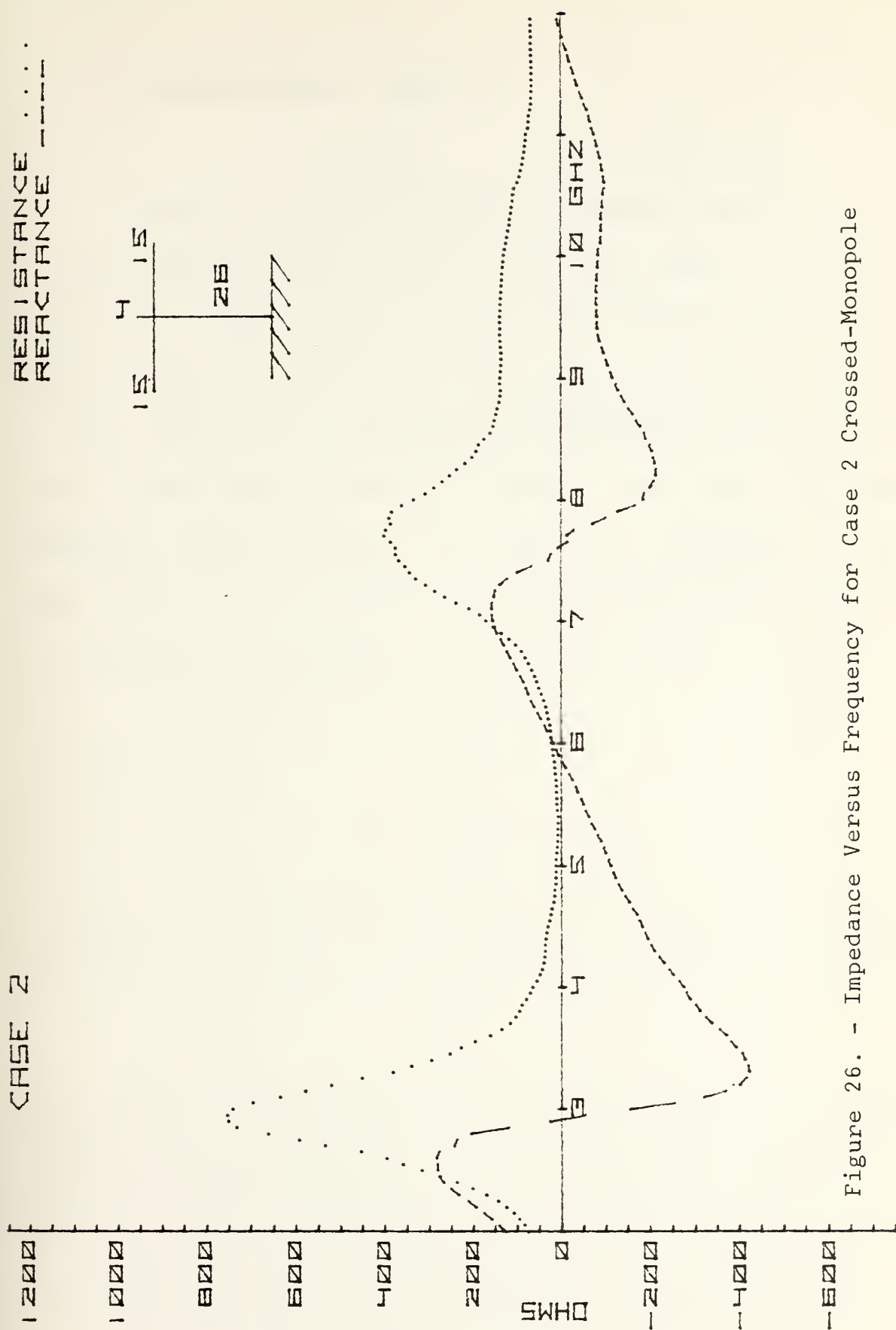


Figure 26. - Impedance Versus Frequency for Case 2 Crossed-Monopole

3. Crossed-Monopole Case 3

Figure 27 is a plot of the impedance characteristics for the crossed-monopole Case 3. The arms remain 15 mm long but were lowered 7.5 mm from the top of the 30 mm vertical member. When compared to the Case 1 curves there is a shift to the right of all resonant and antiresonant points about equal to the factor by which the sum of the arm plus the vertical member below the cross has decreased. The capacitance factors described above continue to increase due to the lower arm position.

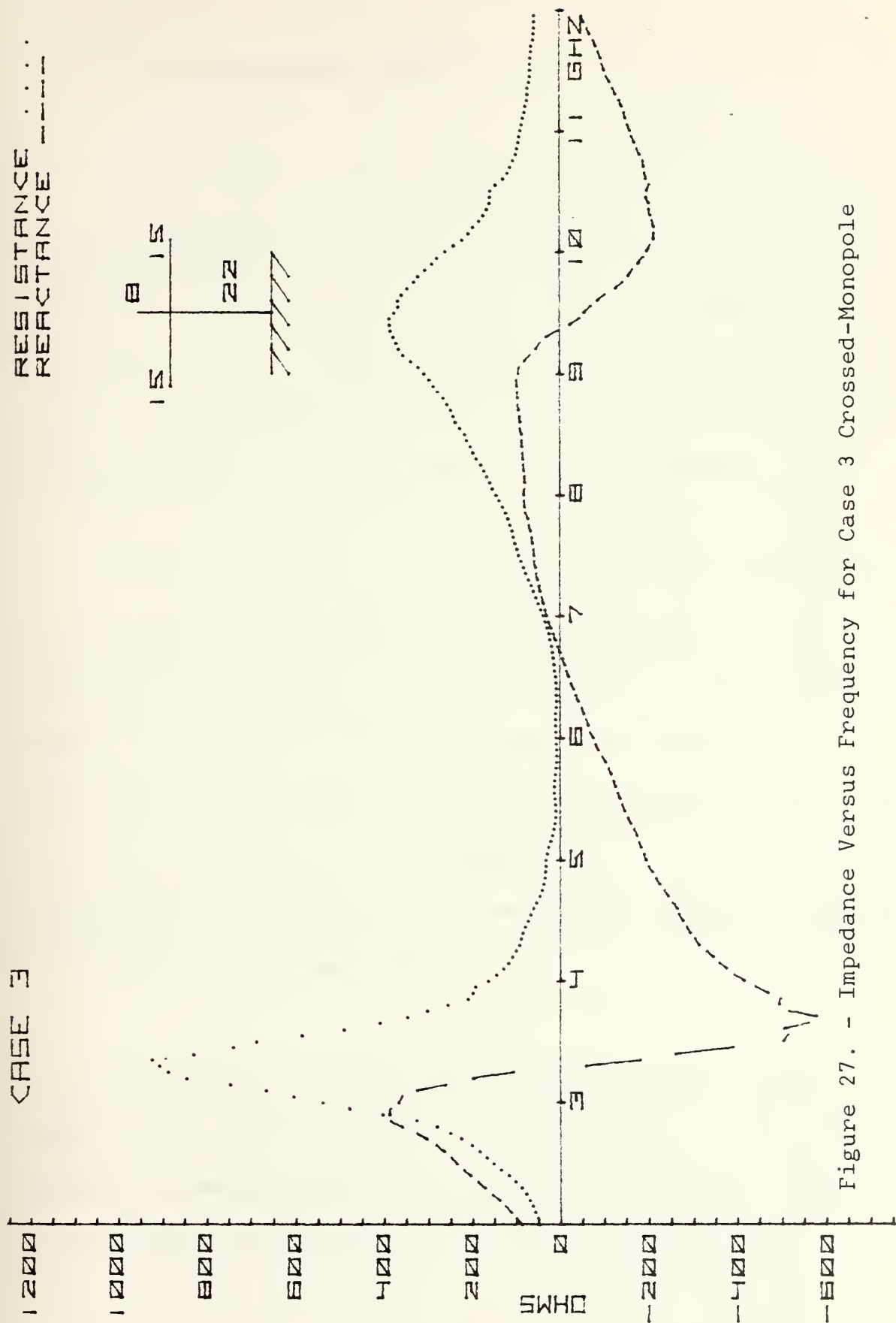


Figure 27. - Impedance Versus Frequency for Case 3 Crossed-Monopole

4. Crossed-Monopole Case 4

Figure 28 is a plot of the impedance characteristics for the crossed-monopole Case 4. The 15 mm arms are located 11 mm from the top of the 30 mm vertical member. Some distortion occurs in the curves at the first antiresonant peak due to reflections from connector interfaces, and conversion from reflection coefficient to impedance.

When the curves are compared to the previous cases the resonant and antiresonant points continue to be shifted to the right due to the shorter dimension of the vertical member below the cross. The capacitance factors are 3.2, 2.19, and 1.99 for the half-wave, three-quarter-wave, and full-wave resonant and antiresonant points. The factors continue to increase due to the decreased distance between the arms and the ground plane.

In Case 2, 3, and 4 the vertical member above the cross seems to have little observable effect. Some effect should be observed when a minimum on the vertical member's charge distribution is located at the junction. In Case 2 a

charge minimum never occurred at the junction. In Case 3 a charge minimum occurred at the junction at about 9.2 GHz or near the full-wave antiresonant point. When the Case 3 curves are compared to the 30 mm monopole curves the full-wave antiresonant occurs at about the same frequency and has the same shape. In Case 4 the charge minimum occurs at the arm location at about 7 GHz when both the 30 mm monopole and Case 4 crossed-monopole have a resistance minimum and the reactance curve with a small value and positive slope.

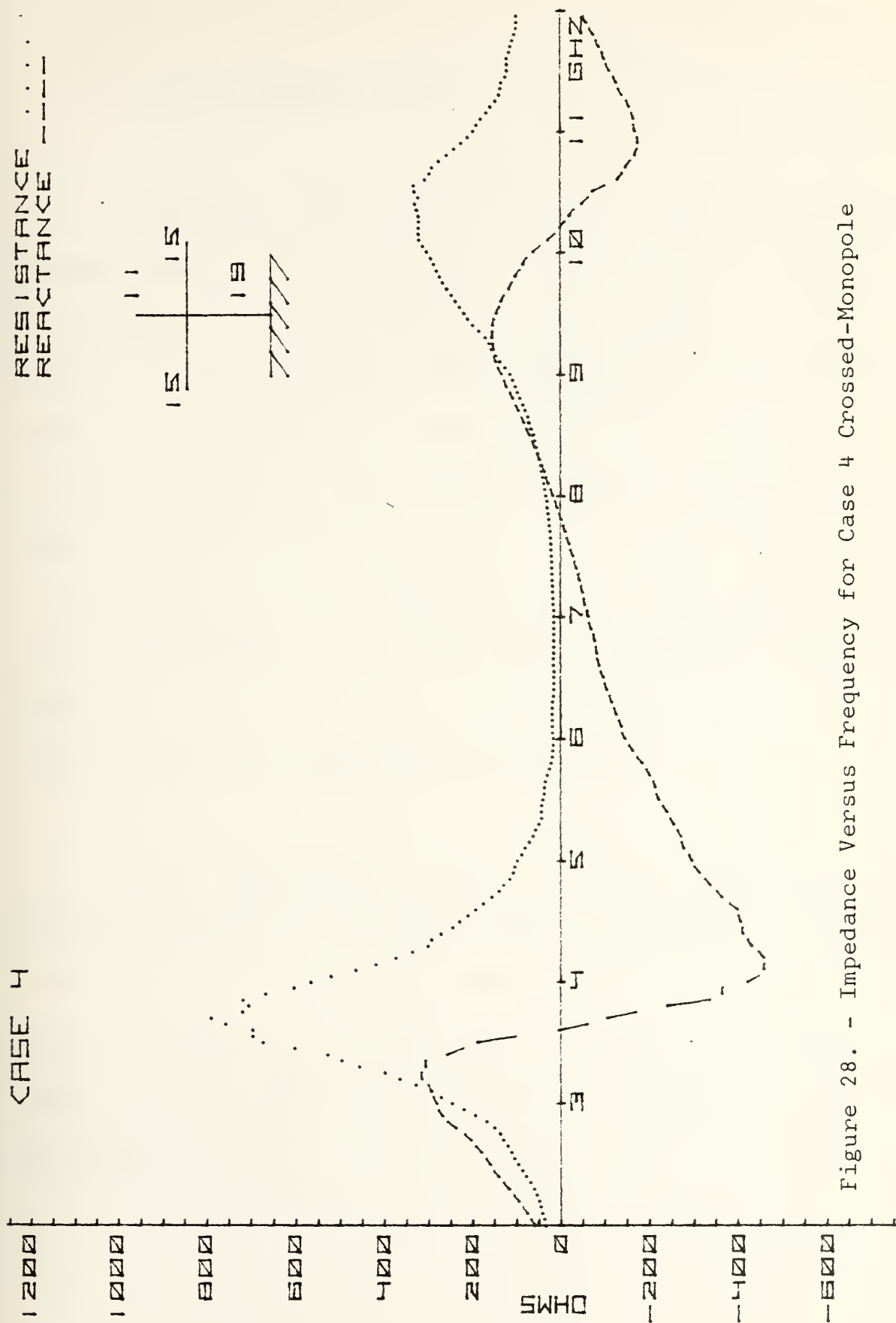


Figure 28. - Impedance Versus Frequency for Case 4 Crossed-Monopole

5. Crossed-Monopole Case 5

Figure 29 is a plot of the input impedance characteristics for the crossed-monopole Case 5. The arms are located at the center of the vertical member, and will cause a charge minimum in the distribution on the vertical member to occur at the arm location at about 4.3 GHz. Due to the location of the charge minimum the curves closely resembles a 30 mm monopole in the area of 3 to 4 GHz, but at 5 GHz there is a large antiresonant peak. This peak is due to the equal length of all three loading elements which when combined with the 15 mm vertical member below the cross forms a high Q antiresonance at this point.

The capacitance factors used in analyzing the previous cases are of little use due to the effects of the vertical member above the cross. This limitation is most noticeable in the 4 to 5 GHz range. However, the continued shift to the right of the full-wave antiresonant point is observable.

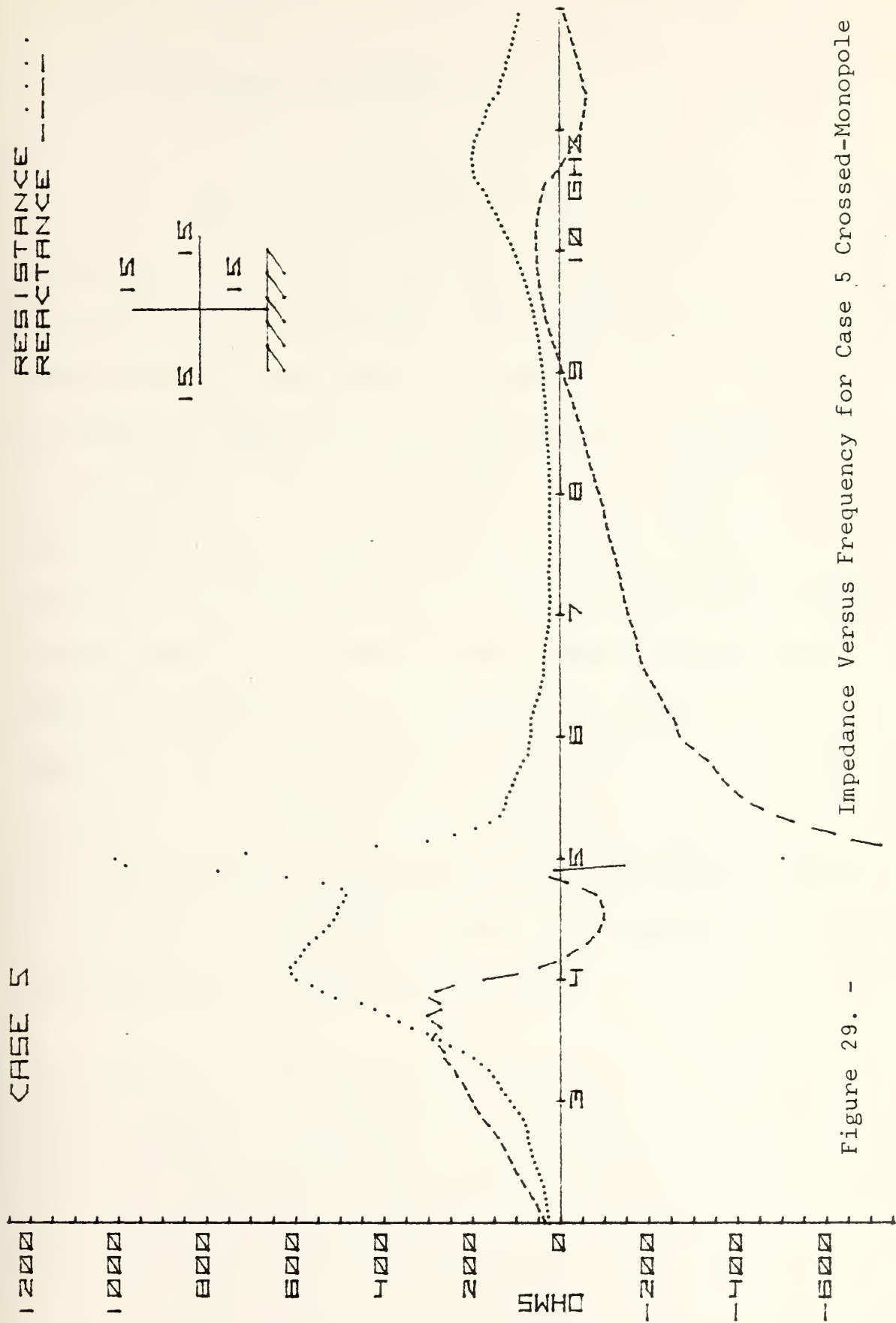


Figure 29. -

6. Crossed-Monopole Case 6

For the crossed-monopole Case 6 the structure used in Case 4 was inverted. This position placed the arms 9.5 mm above the ground plane. The resulting input impedance characteristics are shown in Figure 30. The small antiresonant peaks at 3.5 and 10 GHz are attributed to the vertical member, and occur at points when a minimum in the charge distribution on the vertical member is located at the junction. The large peak at 6.5 GHz is due to the half-wave antiresonance of the arms plus the vertical member below the cross. The distortions of the curves in the 5.5 to 8.5 GHz range are due to the reflections caused by the connector interfaces as discussed earlier. The capacitance factor of 4.17 was calculated at the half-wave antiresonant frequency of 6.4 GHz. This value shows the increase in the capacitance due to lower arm position.

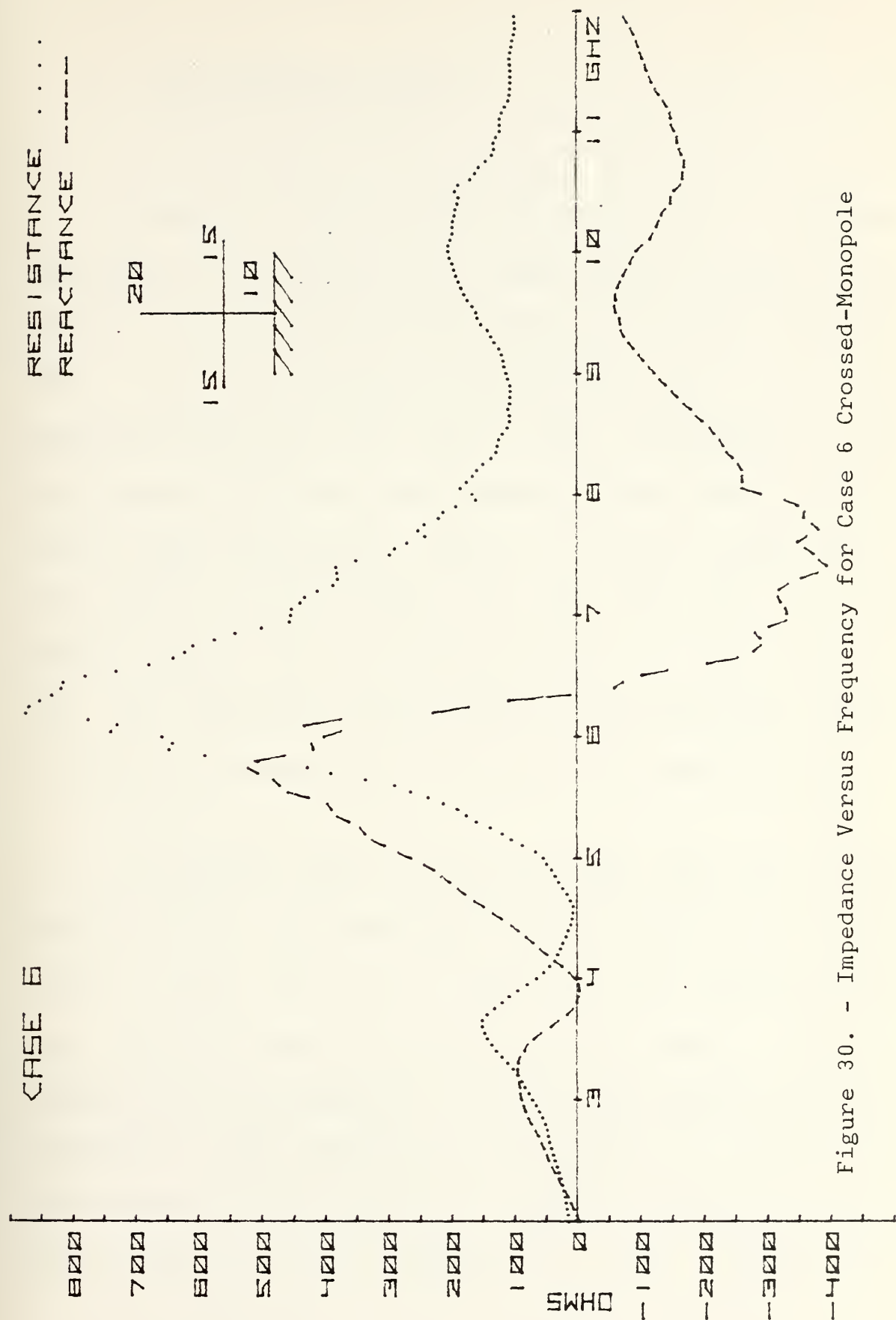


Figure 30. - Impedance Versus Frequency for Case 6 Crossed-Monopole

7. Crossed-Monopole Case 7

Figure 31 is a plot of the input impedance characteristics curves for the crossed-monopole Case 7. The antenna was constructed by inverting the structure used for Case 3 placing the arms 6 mm from the ground plane. The resistance peaks at 3.5 and 10 GHz correspond to the half-wave and full-wave antiresonance of the vertical member and the large antiresonant peak at 7.6 GHz corresponds to the half-wave antiresonance of the arms plus the lower vertical member. The capacitance factor at this point is 7.41 and indicates the relatively large capacitance caused by the short distance from the arms to the ground plane.

In Cases 1 thru 7, 15 mm arms were used with a 30 mm vertical member. The arms were first placed on top of the vertical member and then lowered in each successive case until they were only 6 mm from the ground plane. At each resonant and antiresonant point a capacitance factor was calculated. This factor is the amount by which the capacitance of an equivalent series or parallel resonant circuit would have to increase in order to shift the

resonant frequency from that of a monopole with a height of the vertical member below the cross to that of the crossed-monopole. This factor decreased with increasing frequency due to changes in the charge distribution on the arms and increased as the arms were lowered. The vertical member above the cross may have also effected the capacitance factor in some cases. Since the exact relation between the different parameters effecting the capacitance factor are unknown the effects could not be separated. Only a qualitative analysis could be accomplished. However, the factors were useful in comparing the different cases and will be used in the following cases.

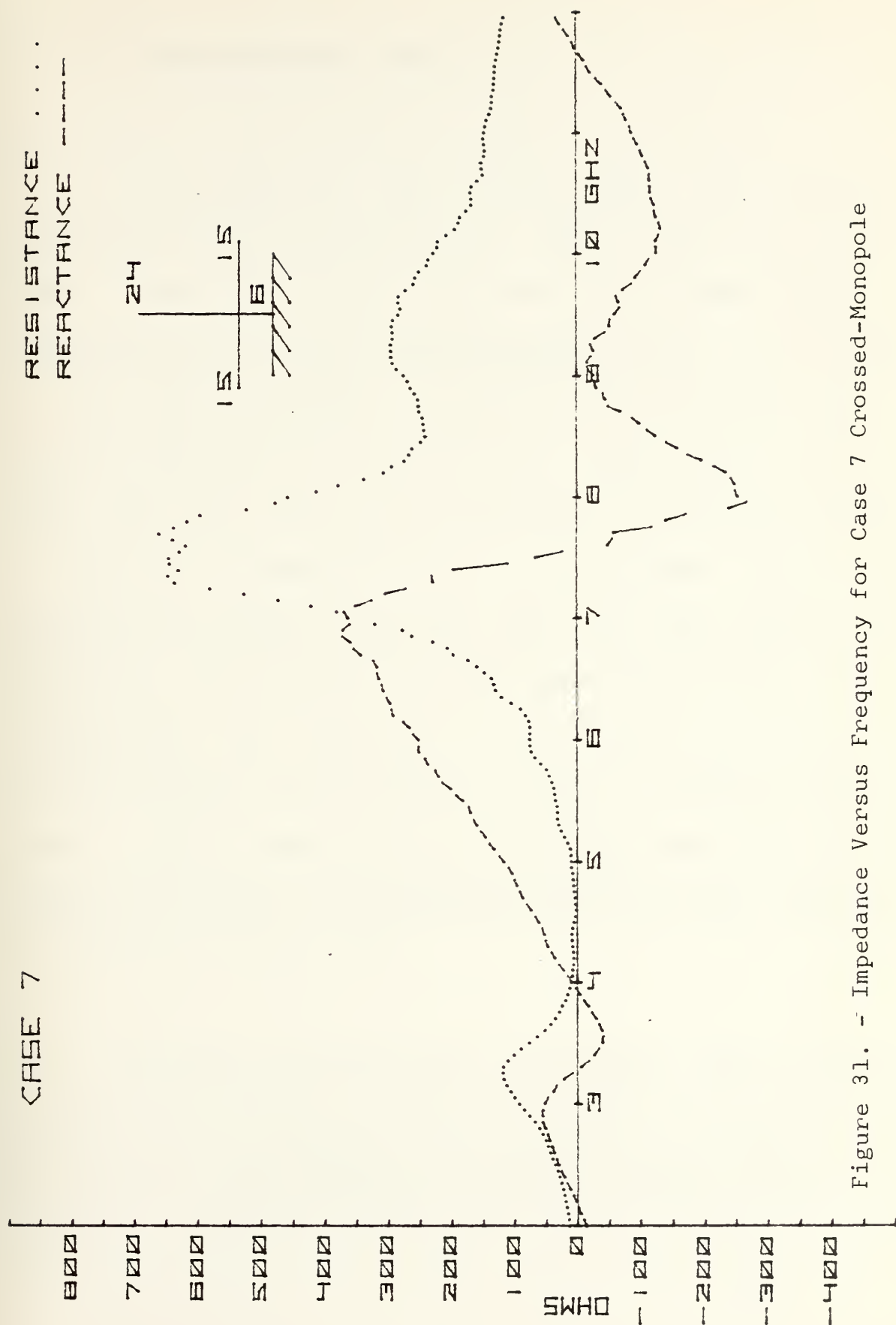


Figure 31. - Impedance Versus Frequency for Case 7 Crossed-Monopole

8. Crossed-Monopole Case 8

The following seven cases differ from the first seven cases in that 12 mm arms are used insted of 15 mm arms. Figure 32 shows the plots of the input impedance characteristics for the crossed-monopole Case 8. As in Case 1 the arms are placed on top of the 30 mm vertical member. When the curves are compared to Case 1 (Figure 25) it can be seen that the resonant and antiresonant points have shifted to the right corresponding to a shorter antenna. Also the capacitance factors which are 1.97, 1.73, and 1.59 for the half-wave, three-quarter-wave, and full-wave resonant points respectively have decreased. Note that the vertical scale has been changed and the peaks in Case 8 are smaller then in Case 1. These results are as anticipated since the shorter arms will decrease the capacitance effect and also decrease the height-to-radius ratio.

In Case 8 an additional antiresonant point occurred at 11.5 GHz. This antiresonant peak did not occur in Case 1. In Case 1 the occurrence of this antiresonant point would require a current minimum and charge maximum at the

junction. But as the charge maximum builds up at the junction the repelling effect of the charges on the vertical member tends to decrease the build-up, and the maximum is not reached. This effect was noted earlier in Case 1 where the capacitance of the arms decreased with increase in frequency but never went to zero.

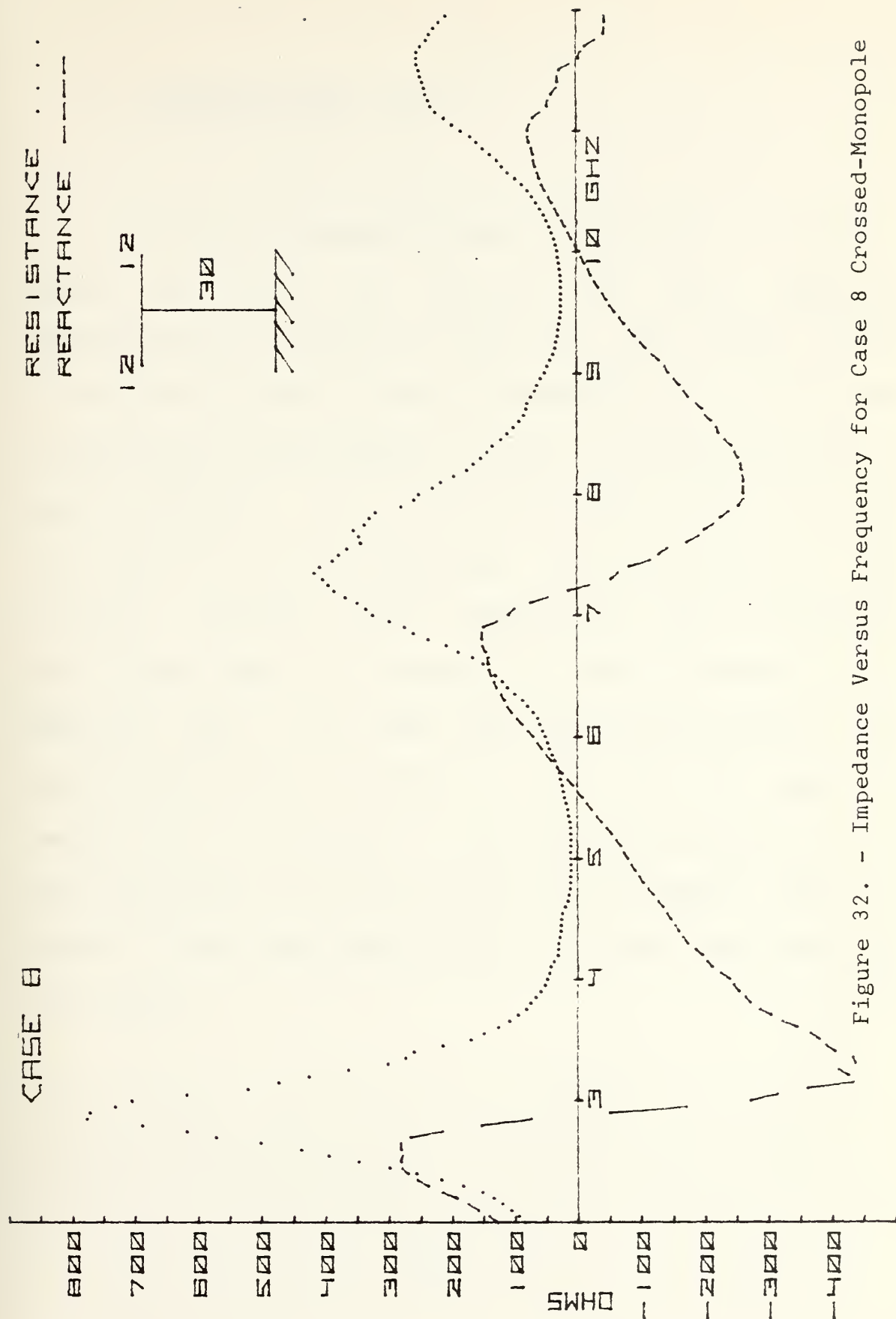


Figure 32. - Impedance Versus Frequency for Case 8 Crossed-Monopole

9. Crossed-Monopole Case 9

The Case 9 crossed-monopole is similar to Case 2 except the arms are shorter. The input impedance characteristics are shown in Figure 33. When these curves are compared to those of Case 2 (Figure 26) one can see that the resonant and antiresonant points have been shifted to a higher frequency. The capacitance factors which are 2.18, 1.84, and 1.63 for the half-wave, three-quarter-wave, and full-wave resonant points respectively have decreased. These comparisons are similar to those obtained when comparing Case 8 to Case 1 and are as anticipated. When Case 9 is compared to Case 8 it can be seen that the resonant and antiresonant points have been shifted to the right, and the capacitance factors have increased. This is similar to the comparison of Case 2 to Case 1 and gives the same results.

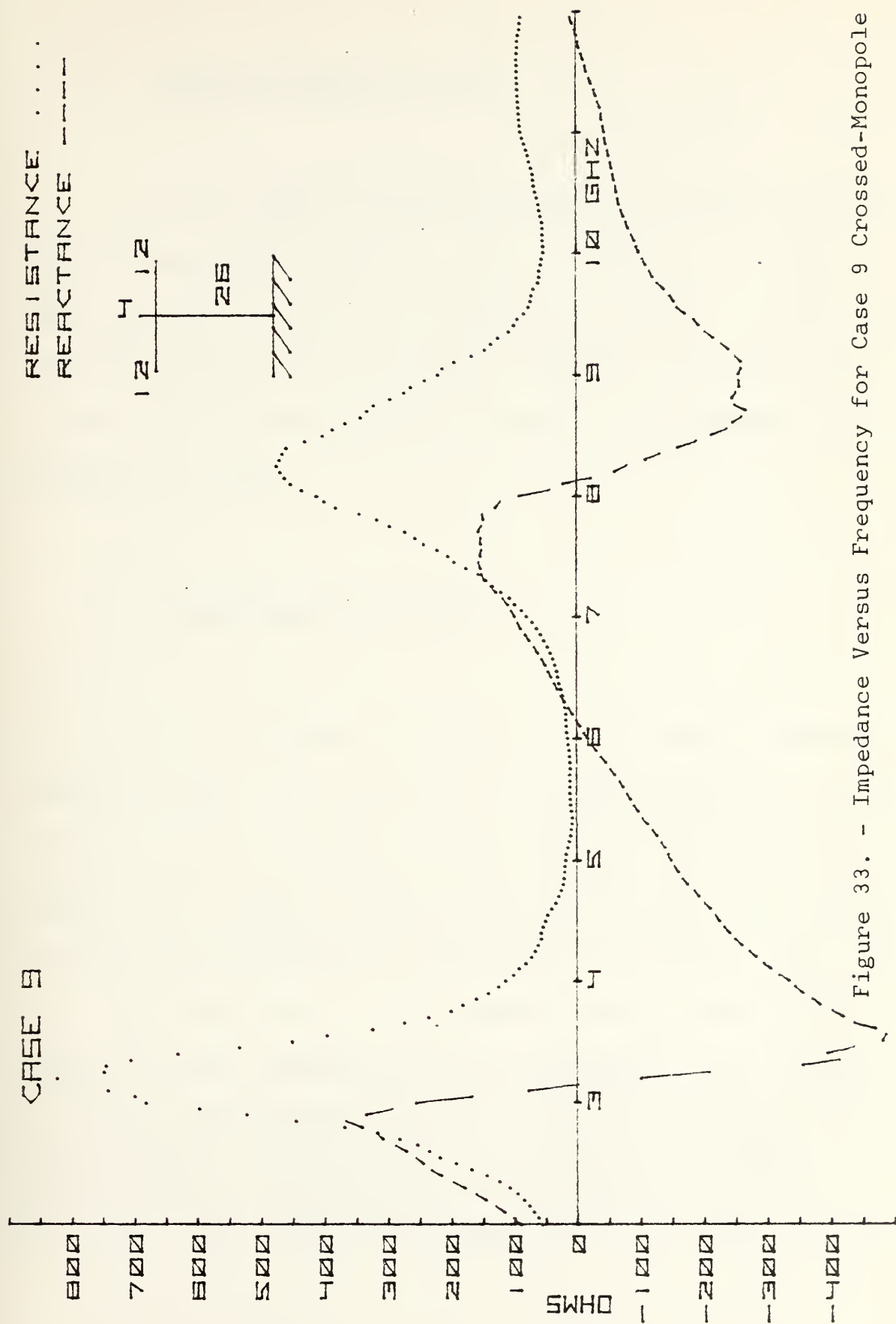


Figure 33. - Impedance Versus Frequency for Case 9 Crossed-Monopole

10. Crossed-Monopole Case 10

For the Case 10 crossed-monopole the arms are 7.5 mm from the top of the vertical member. Figure 34 shows the resulting input impedance characteristic curves. When these curves are compared to the Case 3 (Figure 27) and Case 8 (Figure 32) the results are the same as was obtained in the previous two cases.

11. Crossed-Monopole Case 11

Figure 35 shows the plots for the input impedance characteristics of the Case 11 crossed-monopole. When compared to Case 4 (Figure 28) the resonant and antiresonant points have shifted to the right due to the shorter arms. Also the capacitance factors which are 2.96, 2.11, and 1.91 for the half-wave, three-quarter-wave, and full-wave resonant points respectively have decreased. When compared to Case 8 (Figure 32) the resonant and antiresonant points have shifted to the right due to the decrease distance of the arms plus the vertical member below the cross, and the

capacitance factors have increased because the arms are closer to the ground plane. These results agree with those obtained earlier.

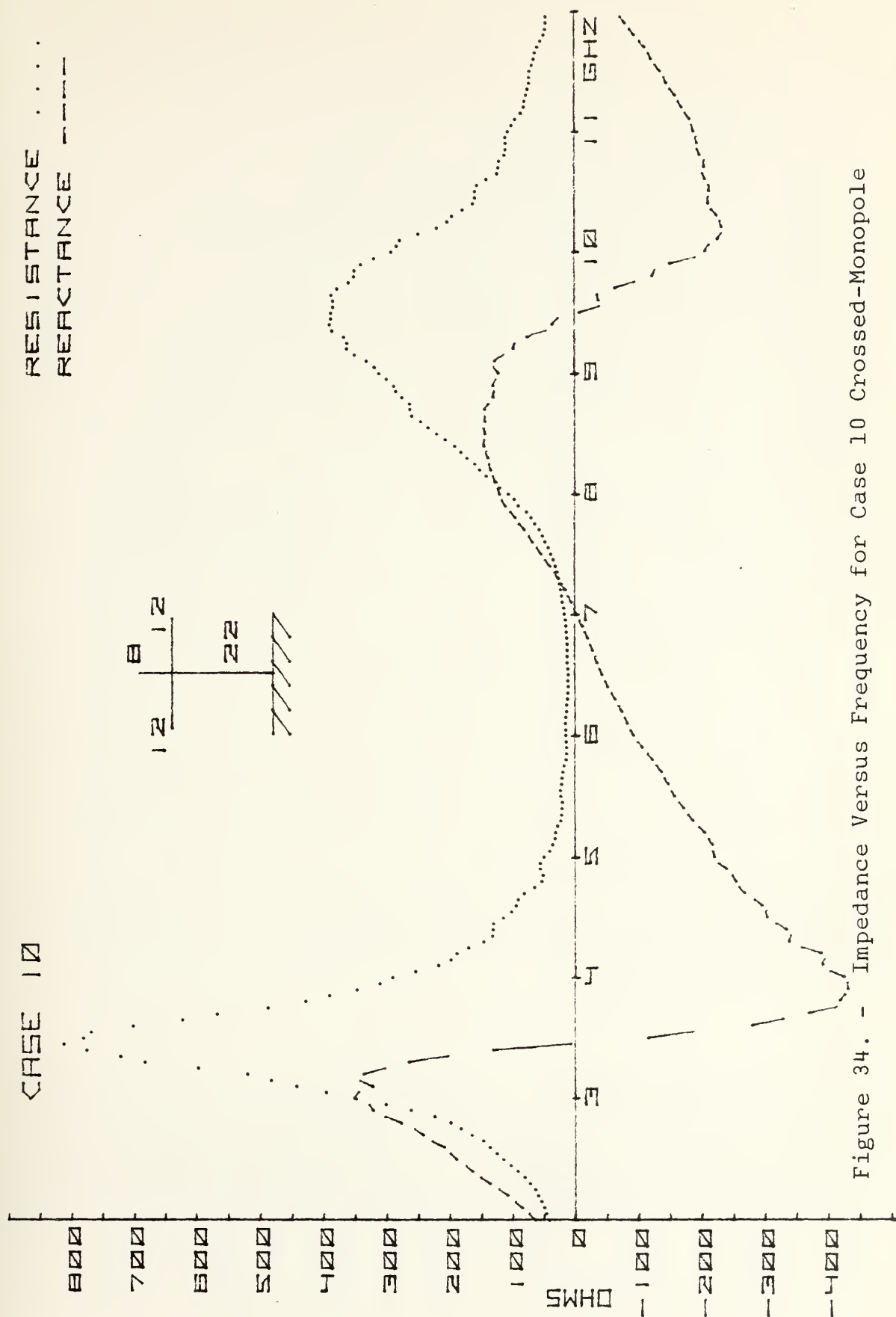


Figure 34. - Impedance Versus Frequency for Case 10 Crossed-Monopole

CASE 11

RESISTANCE
REACTANCE ----

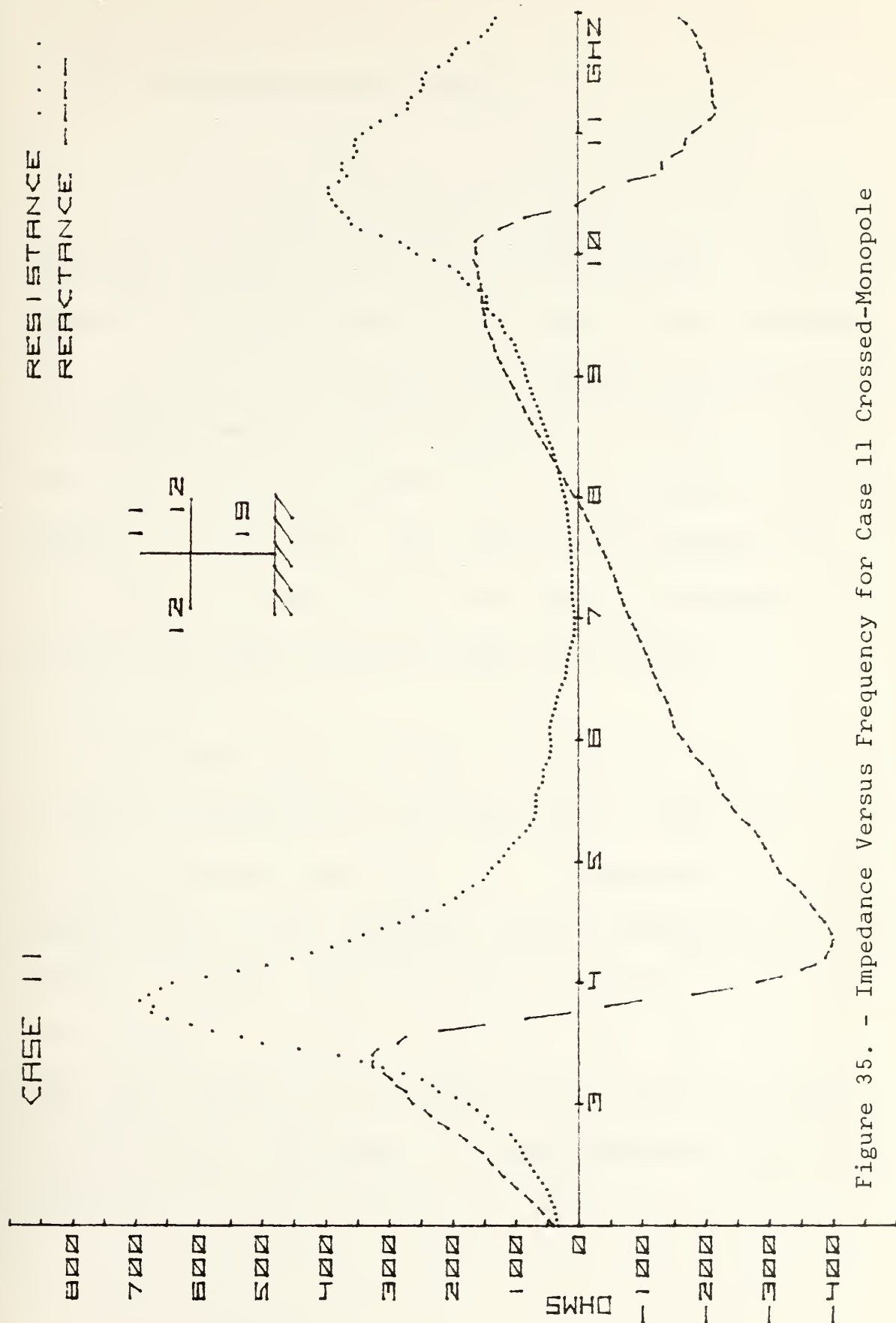
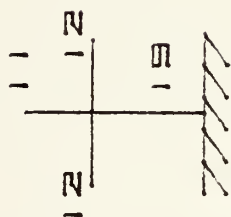


Figure 35. - Impedance Versus Frequency for Case 11 Crossed-Monopole

12. Crossed-Monopole Case 12

For the Case 12 crossed-monopole the 12 mm arms are positioned in the center of the vertical member. The input impedance curves are shown in Figure 36. The antiresonant peak at 4 GHz is caused by the half-wave antiresonance of the vertical member. The large peak at 5.5 GHz is caused by the half-wave antiresonance of the arms plus the vertical member below the cross. The remaining antiresonant peak at 11.8 GHz is caused by the full-wave antiresonance of the arms plus the vertical member below the cross.

As was observed in Case 5 (Figure 39) the effects of the vertical member above the cross can be seen from 3 to 4.5 GHz because there will be a minimum in the charge distribution on the vertical member collocated at the junction at 4 GHz. The curves were compared to Case 5 where longer arms at the same position were used and to Case 8 where arm length is the same but the position is higher. The results are the same as those obtained in similar comparisons

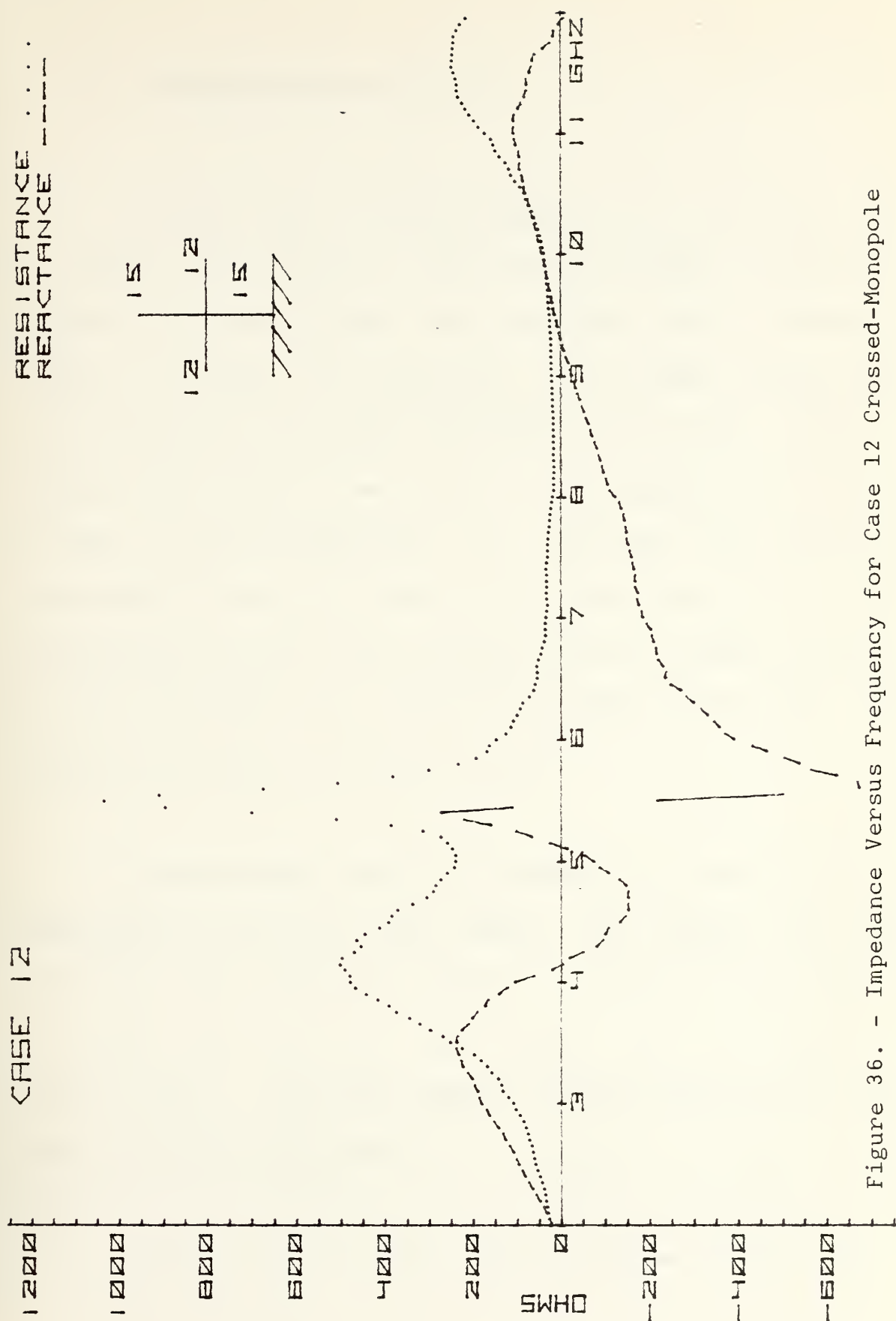


Figure 36. - Impedance Versus Frequency for Case 12 Crossed-Monopole

13. Crossed-Monopole Case 13

For the Case 13 crossed-monopole the structure used in Case 11 was inverted. This position placed the arms 9.5 mm above the ground plane. The resulting input impedance curves are shown in Figure 37. As in Case 6 (Figure 30) charge minimum in the charge distributions on the vertical member will occur at the junction at frequencies of 3.5 and 10 GHz. At these frequencies the half-wave and full-wave antiresonant effects of the vertical member can be observed. Although the full-wave antiresonant point is nearly obscured by the large half-wave antiresonant effect of the arms plus the vertical member below the cross.

Considerable amounts of distortion in the curves are observable in the 6 to 9 GHz range. The source of this distortion was discussed earlier, and it is particularly noticeable when there are broad peaks in the resistance curves due to the large number of data points in the area where the errors are large.

The Case 13 curves were compared to the Case 6

(Figure 30) and Case 8 (Figure 32). The half-wave antiresonant point of the arms plus the vertical member below the cross occurred at a higher frequency due to the shorter arms when compared to Case 6 and due to the smaller vertical member below the cross when compared to Case 8. The capacitance factor at this point was 3.39 which is smaller than in Case 6 due to the shorter arms, but larger than in Case 8 due to the decreased distance to the ground plane.

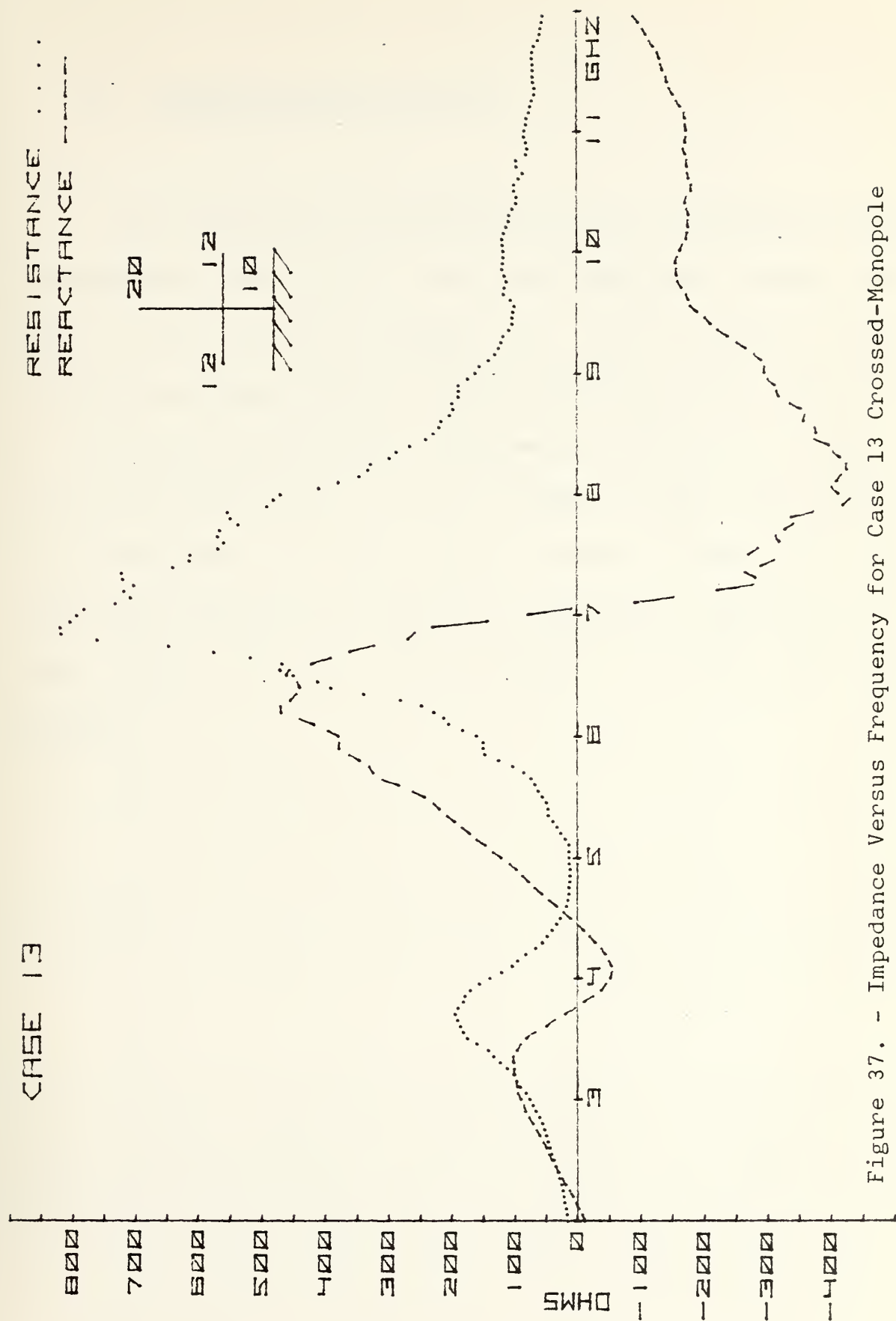


Figure 37. - Impedance Versus Frequency for Case 13 Crossed-Monopole

14. Crossed-Monopole Case 14

The structure used in Case 10 was inverted to make the structure for Case 14. The input impedance curves for Case 14 are shown in Figure 38. The effects of the half-wave antiresonance of the vertical member are observed at 3.5 GHz, and the larger antiresonant point at 8.5 GHz is due to the arms plus the vertical member below the cross. The distortions in the curves beyond 9 GHz limit any conclusions which can be drawn in this area. Comparisons to other cases gives the same results as those obtained earlier.

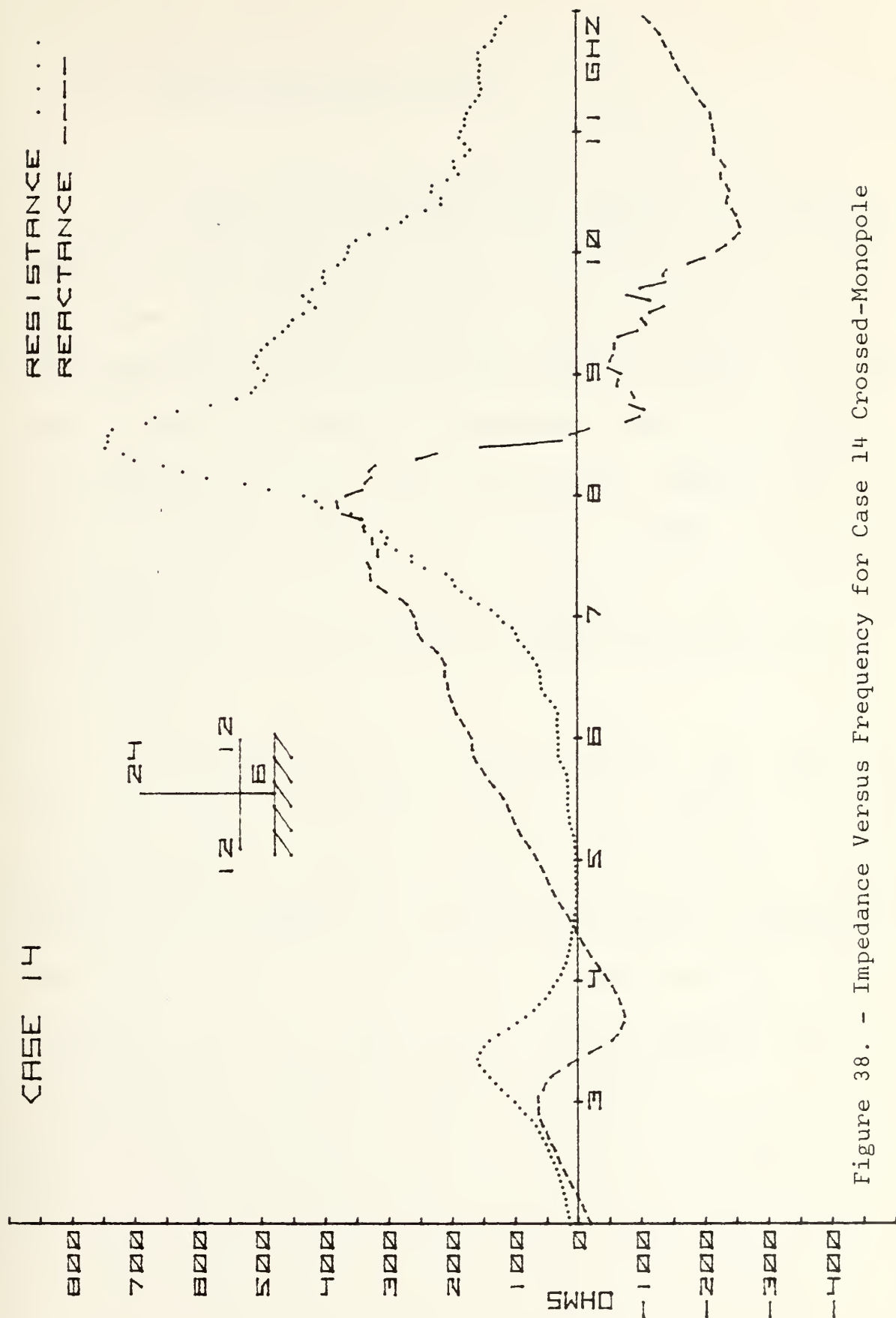


Figure 38. - Impedance Versus Frequency for Case 14 Crossed-Monopole

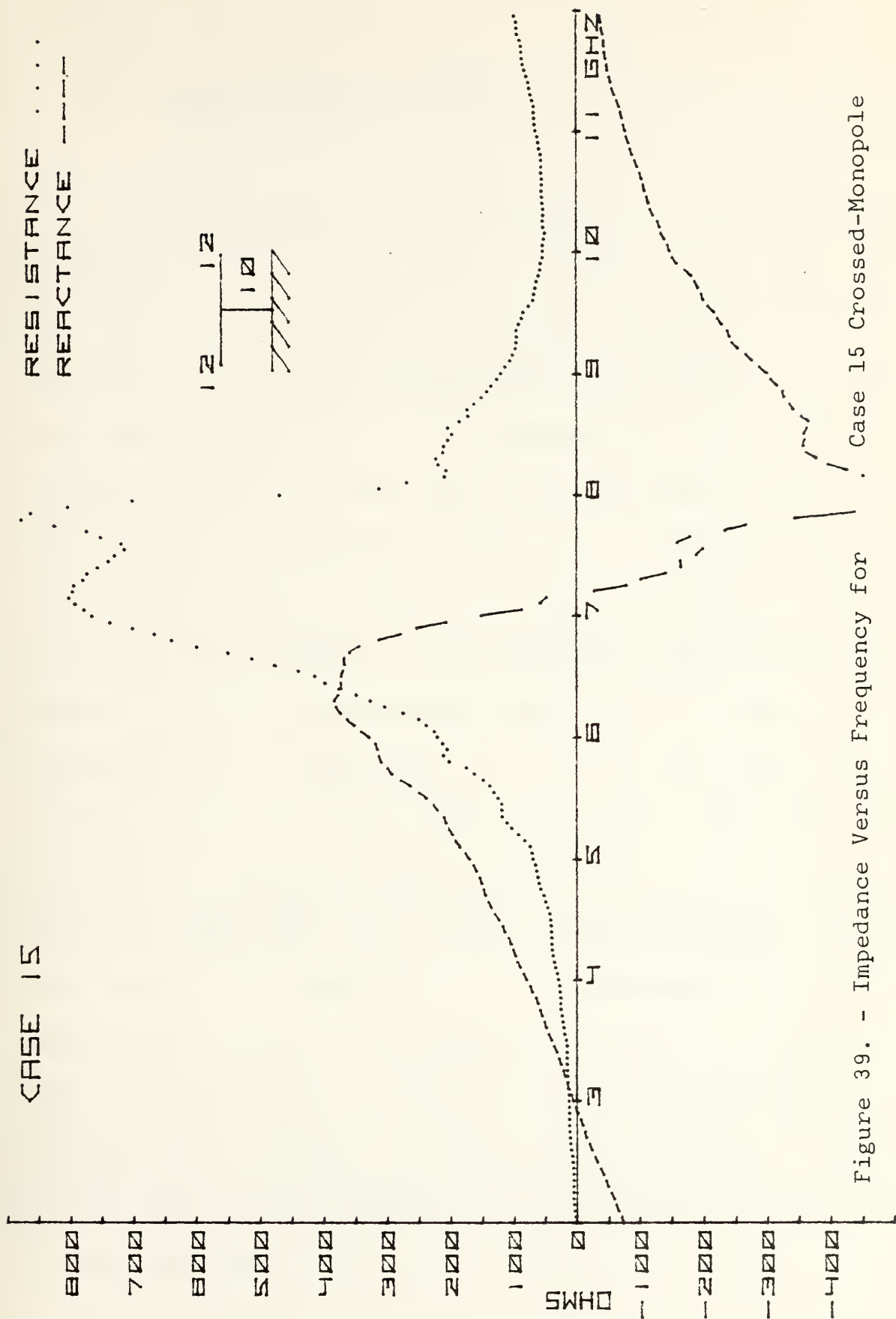
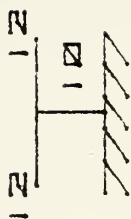
15. Crossed-Monopole Case 15

In order to separate the effects of different members of the crossed-monopole, the vertical member above the cross was removed from the structure used in Case 13. The resulting impedance curves are shown in Figure 39. When these curves are compared to those for Case 13 (Figure 37), it is apparent that the small antiresonant effects at 3.5 and 10 GHz were caused by the vertical member. The larger antiresonant point at 7 GHz which occurs in both cases is due to the arms plus the vertical member below the cross.

In Case 15 there is an appearance of two peaks in the half-wave antiresonant peak. The second peak is probably caused by resonant effects on the arms. These peaks are not observed in the case 13 curves. Although the distortions in this area may have covered the effect, it is believed that the effect of the vertical member above the cross prevented the second peak from occurring.

CASE 15

RESISTANCE
REACTANCE ----



Case 15 Crossed-Monopole

Figure 39. - Impedance Versus Frequency for

16. Crossed-Monopole Case 16

The structure used in the Case 16 crossed-monopole is similar to that used in Case 15 except it has only one arm. The resulting input impedance curves are shown in Figure 40. In comparing the previous cases little was said about the differences in the magnitudes of the different curves since in most cases there was only small changes and these could be explained by changes in the height-to-radius ratio. When comparing Case 16 to Case 15 this is not true. For Case 15 the maximum in the resistance curve is 900 ohms and the half-wave antiresonance occurs at 7.25 GHz which corresponds to a monopole of 17.12 mm. For Case 16 the resistance at the half-wave antiresonance is 700 ohms and occurs at a frequency corresponding to a 19.86 mm monopole which is a lower peak and larger height-to-radius ratio. The change in the magnitude of the resistance curve and the change in the slope of the reactance curve at antiresonance shows that there is a change in the Q of the antiresonance. A change in the Q can not be accounted for by only a change in the capacitance, therefore, the capacitance factors used in comparing previous cases are no longer valid.

CASE 16

RESISTANCE
REACTANCE - - - -

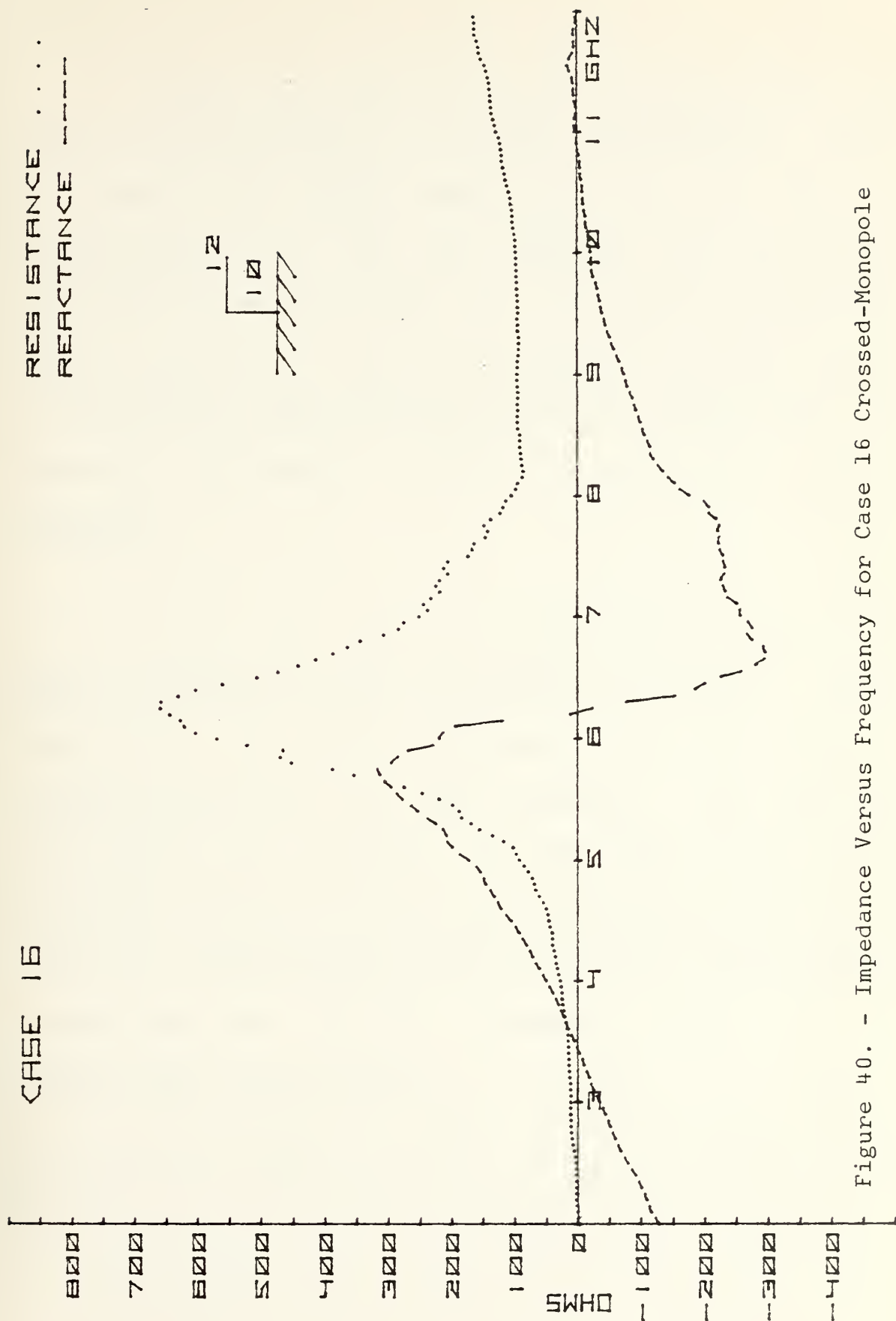


Figure 40. - Impedance Versus Frequency for Case 16 Crossed-Monopole

Figure 41(a) shows the current distribution for the Case 16 crossed-monopole at half-wave antiresonance. Figure 41 (b) shows the current distribution for the Case 15 crossed-monopole at the same frequency. By comparing the two distributions one can see that due to the additional current caused by the second arm in Case 15 the distribution on the vertical member below the cross has shifted, and the half-wave antiresonant point will occur at a higher frequency.

Figure 41(c) shows the current distribution for the Case 16 crossed-monopole at quarter-wave resonance. Figure 41(d) shows the current distribution for the Case 15 crossed-monopole at the same frequency. When the two distributions are compared the additional current of the second arm causes the quarter-wave resonance for Case 16 to occur at a lower frequency than for Case 15. This analysis agrees with the measured impedance curves in the quarter-wave resonance area.

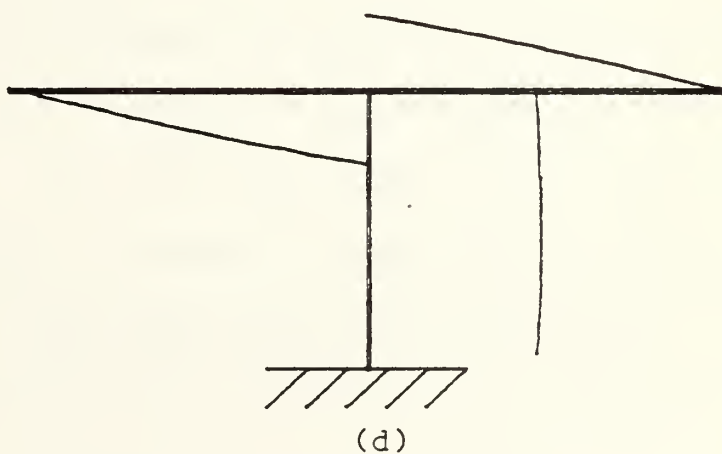
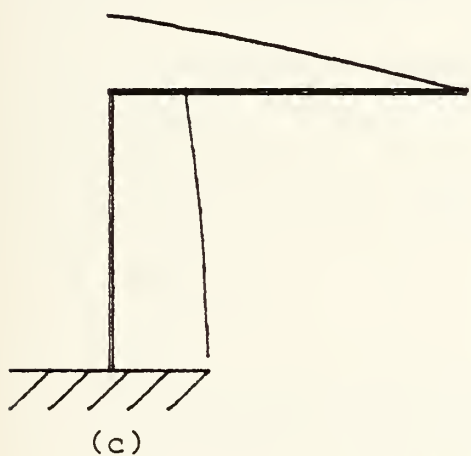
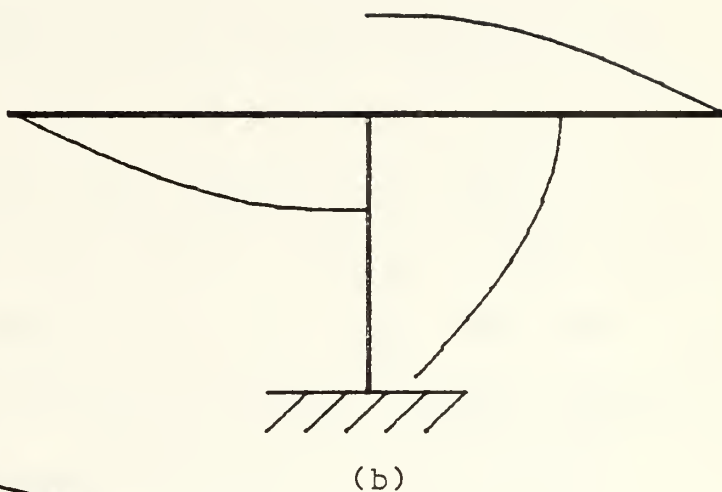
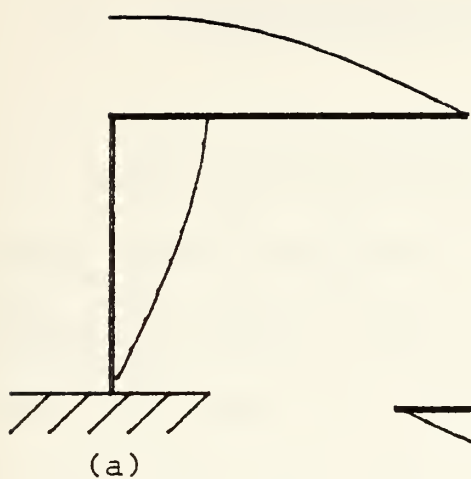


Figure 41. - Current Distribution for
Case 15 and Case 16 Crossed-Monopole

17. Crossed-Monopole Case 17

For the Case 17 crossed-monopole the 9.5 mm vertical member below the cross is loaded with three elements all of different lengths. The resulting input impedance curves are shown in Figure 42. Case 6 (Figure 30) and Case 13 (Figure 37) have the arms at the same position with both arms 15 mm long for Case 6 and 12 mm long for Case 13. When the three sets of curves are compared one can see that the large half-wave antiresonant point for Case 17 occurs between the half-wave antiresonant points for Case 6 and Case 13. Also the capacitance factor at this point which is 4.04 for Case 17 is larger than the 3.39 for case 13 and smaller than the 4.17 for Case 6.

The smaller antiresonant points at 3.5 and 10 GHz are due to the vertical member and are observable on all three sets of curves. The additional effect at 4.5 GHz seen on the case 17 curves is caused by resonance on the total arm of length 27 mm. This effect was not seen in Case 6 or Case 13 because it was covered by the larger antiresonant points.

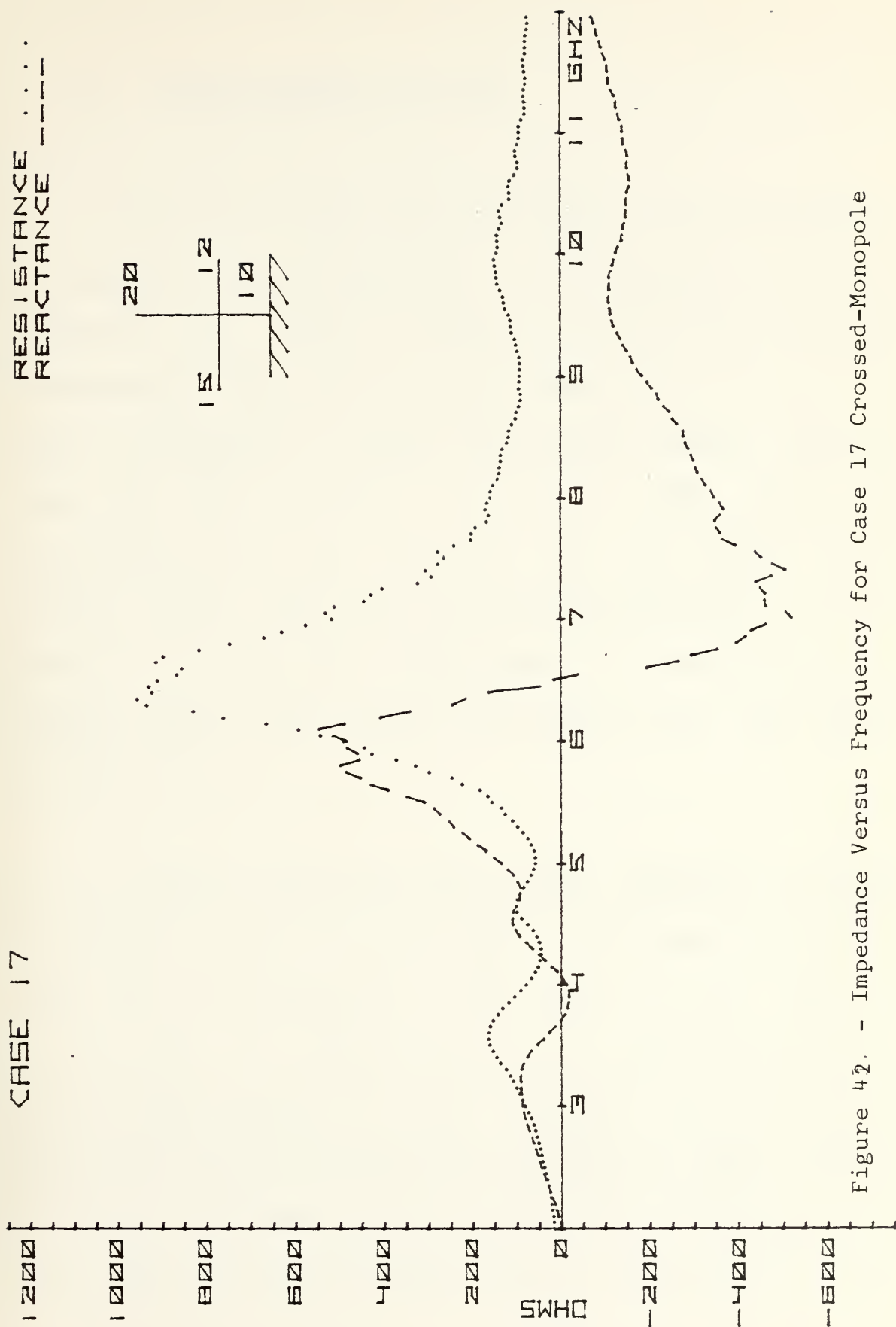


Figure 42. - Impedance Versus Frequency for Case 17 Crossed-Monopole

18. Crossed-Monopole Case 18

Figure 43 shows the input impedance characteristics for the Case 18 crossed-monopole. The crossed-monopole was constructed by placing a single 12 mm arm 9.5 mm above the ground plane. When the curves are compared to those for Case 16 (Figure 40) where the vertical member above the cross has been removed it can be seen that the antiresonances at 3.5 and 9.5 GHz are caused by the vertical member. The peak in the resistance curve at 6.25 GHz is the half-wave antiresonance of the arm plus the vertical member below the arm and occurs at the same place in both plots.

When the curves for Case 18 are compared to those for Case 13 (Figure 37) the shift in the large antiresonant point due to the summation of the current at the junction can be seen. As discussed earlier the capacitance factors are no longer useful due to the change in the Q , however, the left shift in the antiresonant point for Case 18 may be caused by an increase in inductance. The arm forms a half loop with the vertical member which is canceled in the case

with two arms but may add inductance in the case of a single arm. Also the effects of the vertical member are more noticeable due to the decreased effect of the single arm when compared to the antenna with two arms.

CASE 18

RESISTANCE
REACTANCE - - - -

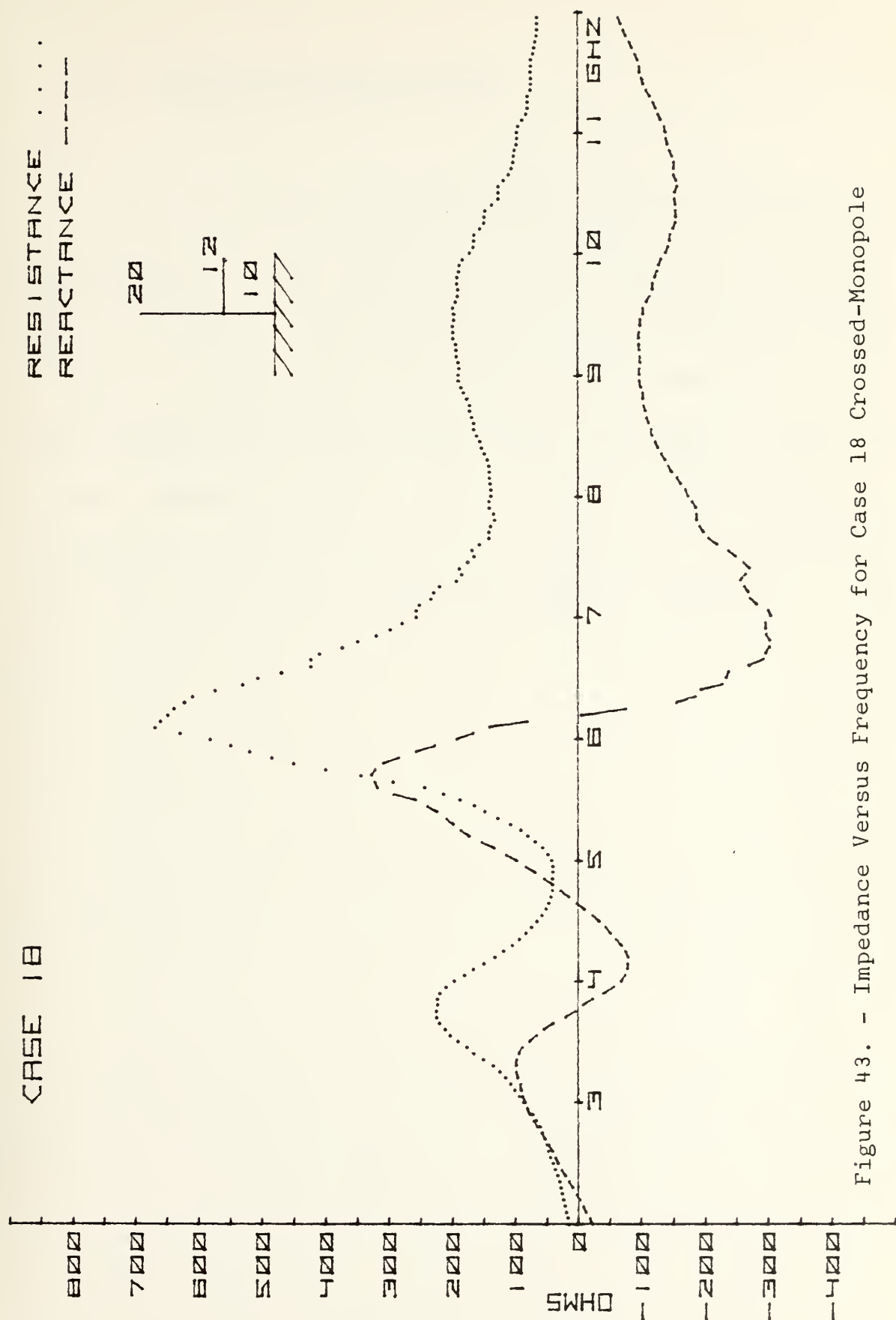
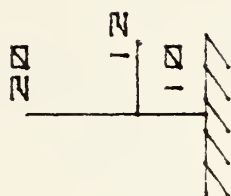


Figure 43. - Impedance Versus Frequency for Case 18 Crossed-Monopole

19. Crossed-Monopole Case 19

For Case 19 a single arm was placed 19 mm above the ground plane. The resulting input impedance curves are shown in Figure 44. When these curves are compared to those of Case 11 (Figure 35) where two arms are used, one can see that the half-wave antiresonant point for Case 19 occurs at a lower frequency than for Case 11 due to the effects of the additional current at the junction caused by the second arm. Also the peak of the resistance curve is smaller for Case 19.

CASE 19

RESISTANCE
REACTANCE ----

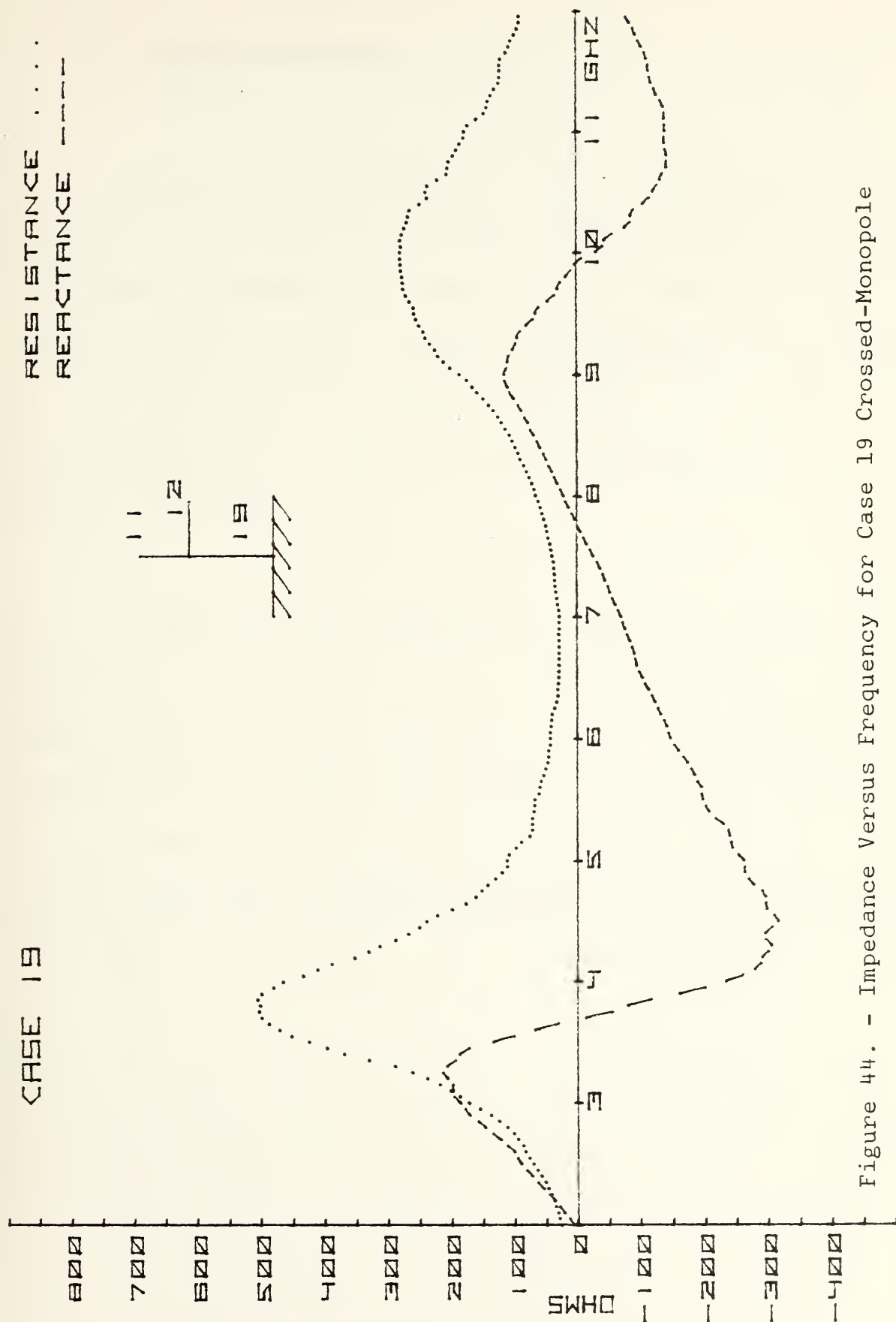


Figure 44. - Impedance Versus Frequency for Case 19 Crossed-Monopole

20. Crossed-Monopole Case 20

Crossed-monopole Case 20 has a single arm 7.5 mm from the top of the 30 mm vertical member. Figure 45 shows the input impedance characteristics for Case 20. As was seen for Case 19, when compared to a structure with two arms at the same position (Case 10, Figure 34) the half-wave antiresonant point occurs at a higher frequency and has a smaller magnitude.

When Case 20 is compared to Case 19 (Figure 44) which has a single arm at a lower position the circuit models used earlier can again be employed. The resonant and antiresonant points for Case 19 occur at a higher frequency, and the capacitance factors which are 3.04, 2.22, and 2.09 for the half-wave, three-quarter-wave, and full-wave points are larger than the 2.58, 1.94, and 1.82 for Case 20.

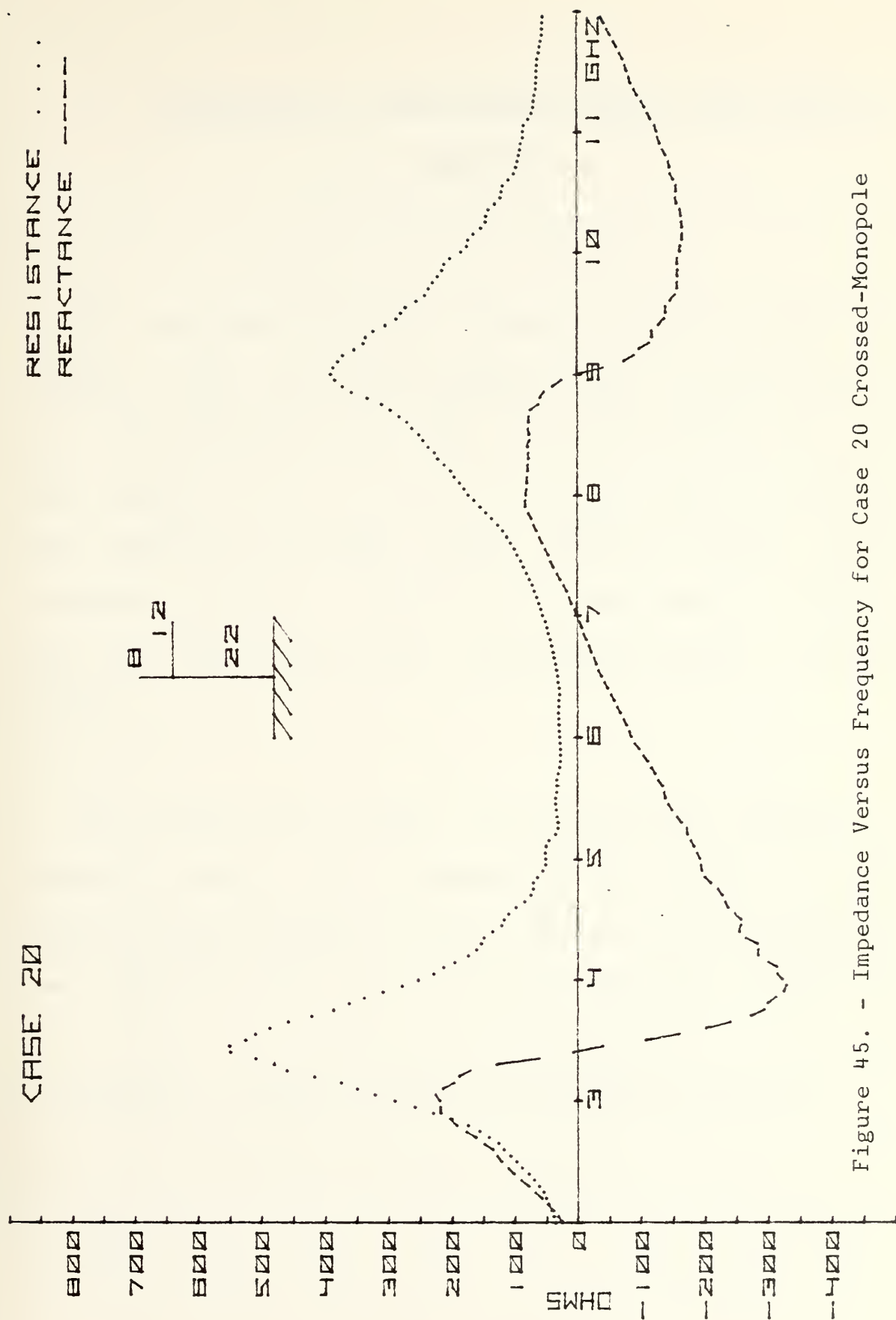


Figure 45. - Impedance Versus Frequency for Case 20 Crossed-Monopole

VI. COMPARISON OF EXPERIMENTAL RESULTS WITH NUMERICAL ANALYSIS

The Antennas-Scatterers Analysis Program (ASAP) [McCormack, 1974] was used to generate input impedance curves for a 30 mm monopole and a Case 13 crossed-monopole. The ASAP program uses the method of moments [Harrington 1968] with piecewise-sinusoidal bases function applied using Galerkin's method. The program was developed by modifying the Ohio State University Antennas-Scatterers Analysis Program.

The program has no means of automatically scanning a frequency range. Each impedance point required recycling the program and a separate data card for each frequency. The impedance points were calculated for every 200 MHz from 2 to 12 GHz. The resulting data was entered in the HP 9821 A calculator and then plotted on the HP 9862 A plotter.

A. MONOPOLE

Figure 46 is the plot of the calculated input impedance for a 30 mm monopole obtained using the ASAP program. The frequencies of the resonant and antiresonant points agrees with those of the measured curves and the theoretical curves. However, the magnitude of the curves more closely resembles that of a monopole with height-to-radius ratio of 40 rather than the actual height-to-radius ratio of 60. The cause of this error is unknown. The limit of the radius to wavelength ratio for the program was exceeded above 6.6 GHz and the data above this frequency may be in error.

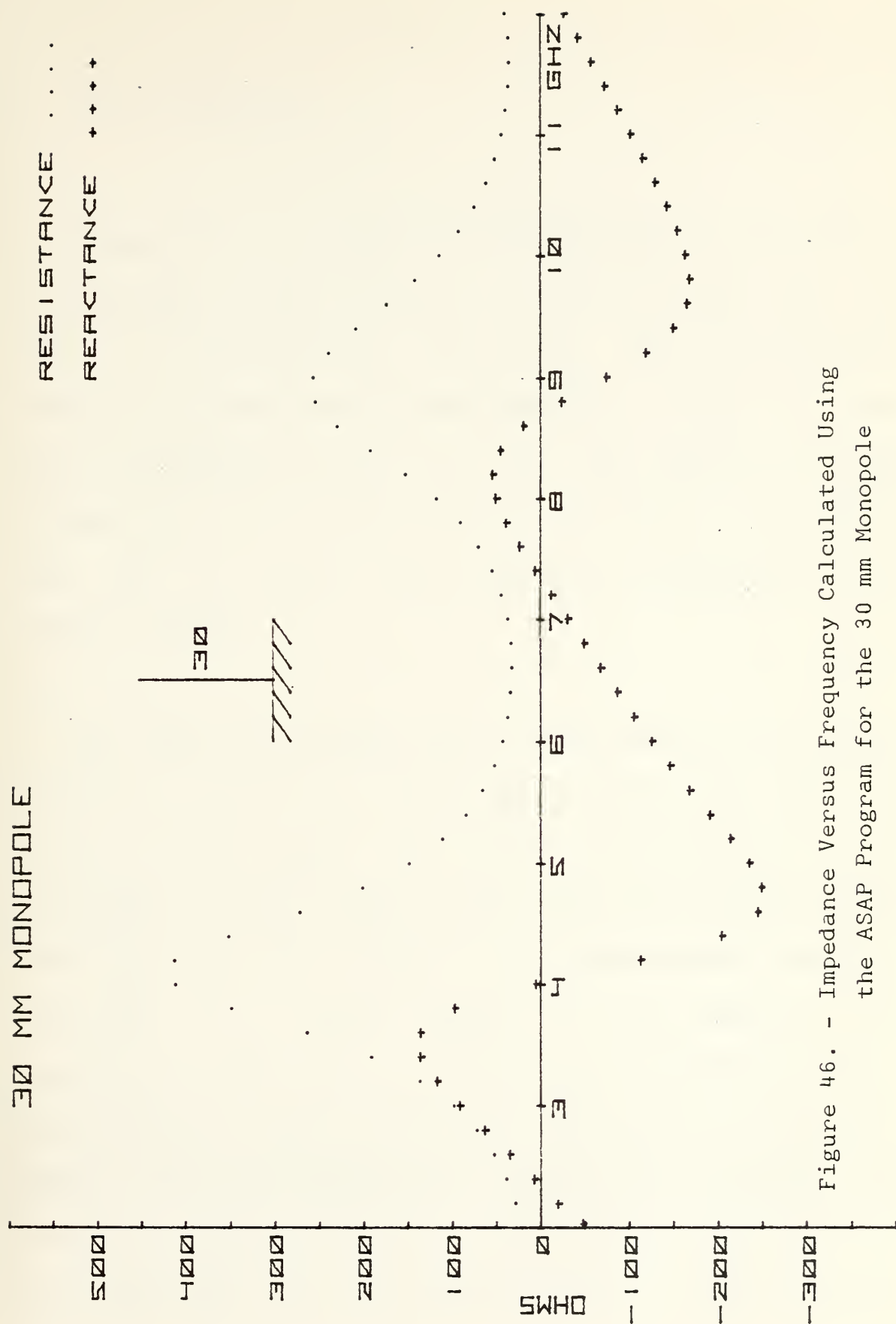


Figure 46. - Impedance Versus Frequency Calculated Using the ASAP Program for the 30 mm Monopole

B. CROSSED-MONOPOLE

Figure 47 is a plot of the calculated impedance for a crossed-monopole with the same dimension as those for the Case 13 crossed-monopole used above. When the curves are compared to those obtained experimentally (Figure 37) the first antiresonant point at 3.75 GHz occurs at the same frequency and has the same magnitude on both sets of curves. This peak is due to the half-wave antiresonance of the vertical member.

The large antiresonant point in the center of the curves is due to the half-wave antiresonance of the arms plus the vertical member below the cross. In the computer curves this point occurs at about 6.2 GHz while the measured curves show the point at 7 GHz. At this antiresonant frequency there will be a charge maximum at the junction. The computer program has no provisions to account for charge accumulation at the junction, and this error is probably the reason for the difference in the two sets of curves. The full-wave antiresonant point of the vertical member is also not observable on the computer curves. This difference

maybe due to the violation of the radius-to-wavelength ratio.

CASE 13 CROSSED-MONOPOLE

RESISTANCE
 REACTANCE ++++

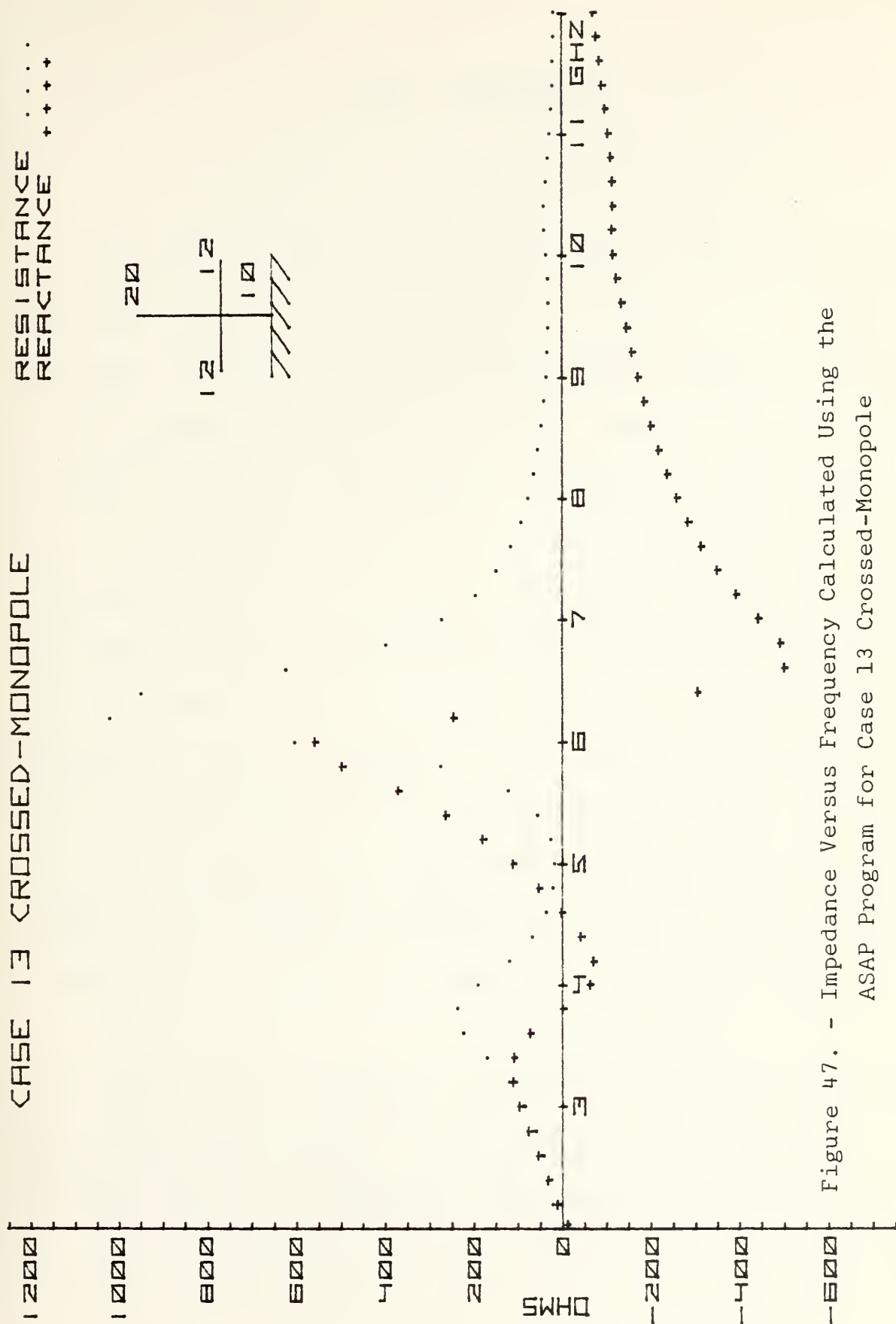


Figure 47. - Impedance Versus Frequency Calculated Using the
 ASAP Program for Case 13 Crossed-Monopole

VII. CONCLUSION

The additon of a cross at the top of a monopole alters the input impedance characteristics to that of a taller monopole. Lowering the cross decreased the effective height of the antenna. Shortening the arms also decreased the effective height. The apparent increase in the height of the monopole due to the cross was found to be a function of frequency due to the change in the charge distribution on the arms. When a crossed-monopole with one arm was compared to a crossed-monopole with two arms it was found that the additional arm increased the effective height at quarter-wave resonance but decreased the effective height at half-wave antiresonance. This effect is caused by a phase shift in the current distribution on the lower vertical member due to the additional current of the second arm.

By the use of frequency scaling the data given in this report can be applied to crossed-monopole antennas of various sizes. A predefined input impedance characteristic may also be approximated by the proper placement of arms of

suitable length.

The results of the numerical analysis shows errors in the impedance curves because charge accumulation at the junction was not accounted for. Also, due to the thin wire approximation used in the program the accuracy of the results at high radius-to-wavelength is limited.

LIST OF REFERENCES

1. Burton, R. W., "The Crossed-Dipole Structure of Aircraft in an Electromagnetic Pulse Environment," Electromagnetic Noise, Interference and Compatibility Advisory Group for Aerospace Research and Development (AGARD) NATO, October 1974.
2. Burton, R. W. and King, R. W. P., "Measured Currents and Charges on Thin Crossed Antennas in a Plane-Wave Field", IEEE Transaction on Antennas and Propagation, v. AP-23, No. 5, p. 657-664, September 1975.
3. Hewlett-Packard Application Note 117-1, Microwave Network Analyzer Applications, p. 8.7-8.9, June 1970.
4. Harrington, R. F., Field Computation by Moment Methods, p. 5-19, Macmillan Company, 1968.
5. Jordan, E. C. and Balmain, K. G., Electromagnetic Waves and Radiating Systems, p. 566-567, Prentice-Hall, Inc., 1968.
6. King, D. D., "Measured Impedance of Cylindrical

Dipoles", Journal of Applied Physics, v. 17, p. 844, 1946.

7. King, R. W. P. and Wu, T. T., " Analysis of Crossed Wires in a Plane-Wave Field", IEEE Transactions on Electromagnetic Compatibility, v. EMC-17, p. 255-265, November 1975.
8. Mc Dowell, E. J., Charge and Current Distributions on, and Input Impedance of Moderately Fat Transmitting Crossed-Monopole Antennas, M.S. E.E. Thesis, Naval Postgraduate School, Monterey, California, March 1976.
9. Mc Cormack, J. W., Antennas-Scatterers Analysis Program, Electrical Engineer Thesis, Naval Postgraduate School, Monterey California, December 1974

INITIAL DISTRIBUTION LIST

No. Copies

- | | | |
|----|--------------------------------------|----|
| 1. | Defense Documentation Center | 2 |
| | Cameron Station | |
| | Alexandria, Virginia 22314 | |
| 2. | Library, Code 0212 | 2 |
| | Naval Postgraduate School | |
| | Monterey, California 93940 | |
| 3. | Department Chairman, Code 62 | 1 |
| | Department of Electrical Engineering | |
| | Naval Postgraduate School | |
| | Monterey, California 93940 | |
| 4. | Professor R. W. Burton, Code 62Zn | 15 |
| | Department of Electrical Engineering | |
| | Naval Postgraduate School | |
| | Monterey, California 93940 | |
| 5. | LT David G. Rundall | 1 |
| | 414 West 3rd St. | |
| | Julesburg, Colorado 80737 | |

6. Post-Doctoral Program 1
RADC-RBC
Rome Air Development Center
Griffiss AFB
New York 13441
7. Mr. Philip Blacksmith 1
Code LZR
Air Force Research Lab.
Laurence G. Hanscom Field
Bedford, Massachusetts 01730
8. Air Force Weapons Laboratory/PRP 2
Kirtland AFB
New Mexico 87117

168136

Thesis

R863

c.1

Rundall

Impedance measurement
of the crossed-monopole
wire structures.

Thesis

R863

c.1

Rundall

Impedance measurement
of the crossed-monopole
wire structures.

168136

thesR863

Impedance measurement of the crossed-mon



3 2768 001 96990 0
DUDLEY KNOX LIBRARY